



Variability and stability of anthropogenic CO₂ in Antarctic Bottom Water observed in the Indian sector of the Southern Ocean, 1978–2018

Léo Mahieu¹, Claire Lo Monaco², Nicolas Metzler², Jonathan Fin², and Claude Mignon²

¹Ocean Sciences, School of Environmental Sciences, University of Liverpool, 4 Brownlow Street, Liverpool L69 3GP, UK

²LOCEAN-IPSL, Sorbonne Université, CNRS/IRD/MNHN Paris, Paris, France

Correspondence: Léo Mahieu (leo.mahieu@liverpool.ac.uk) and Claire Lo Monaco (claire.lomonaco@locean.upmc.fr)

Received: 24 April 2020 – Discussion started: 4 May 2020

Revised: 21 September 2020 – Accepted: 29 September 2020 – Published: 18 December 2020

Abstract. Antarctic Bottom Water (AABW) is known as a long-term sink for anthropogenic CO₂ (C_{ant}), but the sink is hardly quantified because of the scarcity of observations, specifically at an interannual scale. We present in this paper an original dataset combining 40 years of carbonate system observations in the Indian sector of the Southern Ocean (Enderby Basin) to evaluate and interpret the interannual variability of C_{ant} in the AABW. This investigation is based on regular observations collected at the same location (63° E–56.5° S) in the framework of the French observatory OISO from 1998 to 2018 extended by GEOSECS and INDIGO observations (1978, 1985 and 1987).

At this location the main sources of AABW sampled is the low-salinity Cape Darnley Bottom Water (CDBW) and the Weddell Sea Deep Water (WSDW). Our calculations reveal that C_{ant} concentrations increased significantly in the AABW, from an average concentration of 7 $\mu\text{mol kg}^{-1}$ calculated for the period 1978–1987 to an average concentration of 13 $\mu\text{mol kg}^{-1}$ for the period 2010–2018. This is comparable to previous estimates in other Southern Ocean (SO) basins, with the exception of bottom water close to formation sites where C_{ant} concentrations are about twice as large. Our analysis shows that total carbon (C_{T}) and C_{ant} increasing rates in the AABW are about the same over the period 1978–2018, and we conclude that the long-term change in C_{T} is mainly due to the uptake of C_{ant} in the different formation regions. This is, however, modulated by significant interannual to multi-annual variability associated with variations in hydrographic (potential temperature, Θ ; salinity, S) and biogeochemical (C_{T} ; total alkalinity, A_{T} ; dissolved oxygen, O_2) properties. A surprising result is the apparent stability of C_{ant}

concentrations in recent years despite the increase in C_{T} and the gradual acceleration of atmospheric CO₂. The interannual variability at play in AABW needs to be carefully considered in the extrapolated estimation of C_{ant} sequestration based on sparse observations over several years.

1 Introduction

The carbon dioxide (CO₂) atmospheric concentration has been increasing since the start of industrialization (Keeling and Whorf, 2000). This increase leads to an ocean uptake of about a quarter of C_{ant} emissions (Le Quéré et al., 2018; Gruber et al., 2019a). It is widely acknowledged that the Southern Ocean (SO) is responsible for 40 % of the C_{ant} ocean sequestration (Matear, 2001; Orr et al., 2001; McNeil et al., 2003; Gruber et al., 2009; Khatiwala et al., 2009). Ocean C_{ant} uptake and sequestration have the benefit of limiting the atmospheric CO₂ increase but also result in a gradual decrease in the ocean pH (Gattuso and Hansson, 2011; Jiang et al., 2019). Understanding the oceanic C_{ant} sequestration and its variability is of major importance to predict future atmospheric CO₂ concentrations, the impact on the climate and the impact of the pH change on marine ecosystems (de Baar, 1992; Orr et al., 2005; Ridgwell and Zeebe, 2005).

C_{ant} in seawater cannot be measured directly, and the evaluation of the relatively small C_{ant} signal from total inorganic dissolved carbon (C_{T} ; less than 3 %; Pardo et al., 2014) is still a challenge to overcome. Different approaches have been developed in the last 40 years to quantify C_{ant} concentrations in

the oceans. The “historical” back-calculation method based on C_T measurements and preformed inorganic carbon estimates (C^0) was independently published by Brewer (1978) and Chen and Millero (1979). This method has often been applied at the regional and basin scale (Chen, 1982; Poisson and Chen, 1987; Chen, 1993; Goyet et al., 1998; Körtzinger et al., 1998, 1999; Lo Monaco et al., 2005a). More recently, the TrOCA (Tracer combining Oxygen, dissolved Carbon and total Alkalinity) method has been developed (Touratier and Goyet, 2004a, b; Touratier et al., 2007) and applied in various regions including the SO (e.g., Lo Monaco et al., 2005b; Sandrini et al., 2007; Van Heuven et al., 2011; Pardo et al., 2014; Shadwick et al., 2014; Roden et al., 2016; Kerr et al., 2018). Comparisons with other data-based methods show significant differences in C_{ant} concentrations, especially at high latitudes and more particularly in deep and bottom water (Lo Monaco et al., 2005b; Vázquez-Rodríguez et al., 2009; Pardo et al., 2014).

Antarctic Bottom Water (AABW) is of specific interest for atmospheric CO₂ and heat regulation as it plays a major role in the meridional overturning circulation (Johnson et al., 2008; Marshall and Speer, 2012). AABW represents a large volume of water covering a major part of the world ocean floor (Mantyla and Reid, 1995), and its spreading in the interior ocean through circulation and water mixing is a key mechanism for the long-term sequestration of C_{ant} and climate regulation (Siegenthaler and Sarmiento, 1993). AABW formation is a specific process occurring in few locations around the Antarctic continent (Orsi et al., 1999). In short, AABW formation occurs when the Antarctic surface water flows down along the continental shelf. The Antarctic surface water density required for this process to happen is reached by the increase in salinity (S) due to brine release from ice formation and by a decrease in temperature due to heat loss to either the ice shelf or the atmosphere. Importantly, the AABW formation process is enhanced by katabatic winds that open areas free of ice called polynyas (Williams et al., 2007). Indeed, katabatic winds are responsible for an intense cooling that enhances the formation of ice constantly pushed away by the wind, leading to cold and salty surface water in contact with the atmosphere. The variable conditions of wind, ice production, surface water cooling and continental slope shape encountered around the Antarctic continent lead to different types of AABW, and hence the AABW characteristics can be used to identify formation sites.

The ability of AABW to accumulate C_{ant} has been controversial since one can believe that the ice coverage limits the invasion of C_{ant} in Antarctic surface water (e.g., Poisson and Chen, 1987). This is, however, not the case in polynyas, and several studies have reported significant C_{ant} signals in AABW formation regions, likely due to the uptake of CO₂ induced by high primary production (Sandrini et al., 2007; van Heuven et al., 2011, 2014; Shadwick et al., 2014; Roden et al., 2016). However, little is known about the variability and evolution of the CO₂ fluxes in AABW formation regions,

and since biological and physical processes are strongly impacted by seasonal and interannual climatic variations (Fukamachi et al., 2000; Gordon et al., 2010; McKee et al., 2011; Gordon et al., 2015; Gruber et al., 2019b), the amount of C_{ant} stored in the AABW may be very variable, which could bias the estimates of C_{ant} trends derived from datasets collected several years apart (e.g., Williams et al., 2015; Pardo et al., 2017; Murata et al., 2019).

In this context of potentially high variability in C_{ant} uptake at AABW formation sites, as well as in AABW export, circulation and mixing, we used repeated observations collected in the Indian sector of the Southern Ocean to explore the variability in C_{ant} and C_T in the AABW and evaluate their evolution over the last 40 years.

2 Study area

2.1 AABW circulation in the Atlantic and Indian sectors of the Southern Ocean

The circulation in the SO is dominated by the Antarctic Circumpolar Current (ACC) that flows eastward, while the Coastal Antarctic Current (CAC) flows westward (Carter et al., 2008). The ACC and the CAC influence the circulation of the entire water column and generate gyres, which are crucial drivers of SO circulation (Carter et al., 2008). The most important gyres encountered around the Antarctic continent correspond to major AABW formation sites (Fig. 1). The main AABW formation sites are the Weddell Sea, where Weddell Sea Deep Water and Weddell Sea Bottom Water are produced (WSDW and WSBW, respectively; Gordon, 2001; Gordon et al., 2010), the Ross Sea for the Ross Sea Bottom Water (RSBW; Gordon et al., 2009, 2015), the Adélie Land coast for the Adélie Land Bottom Water (ALBW; Williams et al., 2008, 2010) and the Cape Darnley Polynya for the Cape Darnley Bottom Water (CDBW; Ohshima et al., 2013). AABW formation has also been observed in the Prydz Bay (Yabuki et al., 2006; Rodehacke et al., 2007). There, three polynyas and two ice shelves have been identified as Prydz Bay Bottom Water (PBBW) production hotspots from seal tagging and mooring data (Williams et al., 2016). This PBBW flows out of the Prydz Bay through the Prydz Channel and gets mixed with the CDBW. The mix of CDBW and PBBW (hereafter called CDBW) represents significant AABW export (13 % of all AABW export; Ohshima et al., 2013).

The largest bottom water source of the global ocean is the Weddell Sea (Gordon et al., 2001). The exported WSDW is a mixture of the WSBW and Warm Deep Water (WDW). The WDW is a slightly modified Lower Circumpolar Deep Water (LCDW) by mixing with high-salinity surface water when the LCDW enters the Weddell basin (see Fig. 2 in van Heuven et al., 2011). The WSDW mixes with the LCDW during its transit. A part of the WSDW deflecting southward

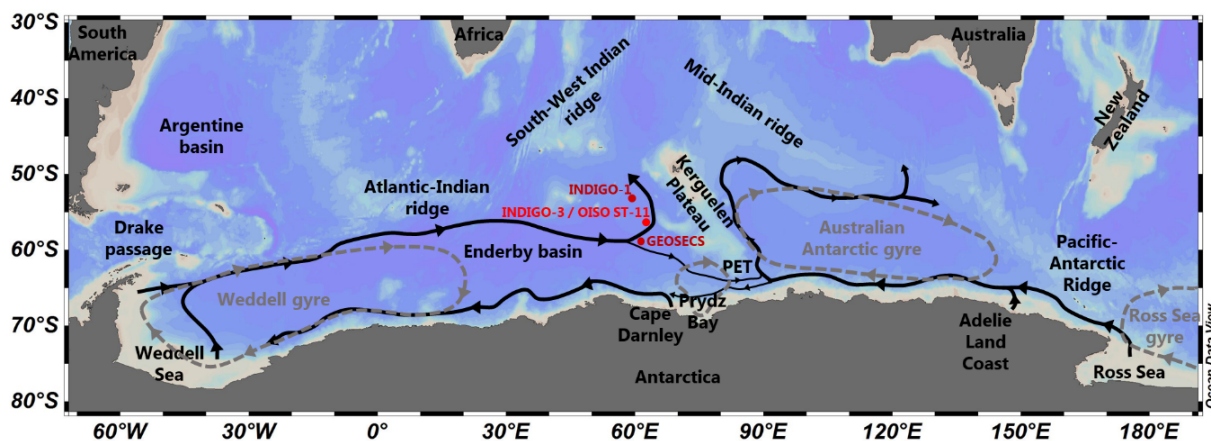


Figure 1. The rough AABW circulation transport paths from the literature (Orsi et al., 1999; Carter et al., 2008; Fukamachi et al., 2010; Williams et al., 2010; Vernet et al., 2019), with geographic indications (black text), main SO gyres (dark yellow text and dashed lines for the approximative locations) and stations considered in this study (red text and dots). PET: Princess Elizabeth Trough. Figure produced with Ocean Data View (Schlitzer, 2019).

with the ACC in the Enderby Basin reaches the northwestern part of the Princess Elizabeth Trough (PET) region (area separating the Kerguelen Plateau from the Antarctic continent), where it mixes with other types of AABW (Heywood et al., 1999; Orsi et al., 1999). The deepest point of the PET is 3750 m, deep enough to allow AABW to flow between the Australian Antarctic Basin and the Enderby Basin (Heywood et al., 1999).

At the east of the PET, the CAC transports a mixture of RSBW and ALBW and accelerates northward along the eastern side of the Kerguelen Plateau (Mantyla and Reid, 1995; Fukamachi et al., 2010) following the Australian–Antarctic gyre, also called the Kerguelen gyre (Vernet et al., 2019). Part of the ALBW–RSBW mixture reaches the western side of the Kerguelen Plateau by the southern part of the PET (Heywood et al., 1999; Orsi et al., 1999; Van Wijk and Rintoul, 2014) and mixes with the CDBW. The mixture of CDBW and ALBW–RSBW flows westward with the CAC and dilutes with the LCDW (Meijers et al., 2010) until it reaches the Weddell gyre (Carter et al., 2008).

2.2 AABW definition

The distinction of water masses is usually performed according to neutral density (γ^n) layers. In the SO, LCDW and AABW properties are generally well defined in the range 28.15–28.27 kg m⁻³ and 28.27 kg m⁻³ to the bottom, respectively (Orsi et al., 1999; Murata et al., 2019). However, to interpret the long-term variability of the properties in the AABW core at our location, we prefer to adjust the AABW definition to a narrow (more homogeneous) layer that we call Lower Antarctic Bottom Water (LAABW), characterized by $\gamma^n > 28.35$ kg m⁻³ (roughly ranging from 4200 to 4800 m; see Fig. 3). This definition corresponds to the AABW characteristics observed at higher latitudes in the Indian SO sector

(Roden et al., 2016). The layer above the LAABW is hereafter called Upper Antarctic Bottom Water (UAABW).

3 Material and methods

3.1 AABW sampling during the last 40 years

Most of the data used in this study were obtained in the framework of the long-term observational project OISO (Ocean Indien Service d’Observations) conducted since 1998 onboard the R. S. V. *Marion Dufresne* (IPEV/TAAF). During these cruises, several stations are visited, but only one station is sampled down to the bottom (4800 m) south of the Polar Front, at 63.0° E and 56.5° S (hereafter denoted OISO-ST11). This station is located in the Enderby Basin on the western side of the Kerguelen Plateau (Fig. 1) and coincides with station 75 of the INDIGO-3 cruise (1987). In our analysis, we included all the data available for the OISO-ST11 location (which has not been sampled during each cruise for logistic reasons). We also included data from station 14 (deepest sample taken at 5109 m) of the INDIGO-1 cruise (1985) and station 430 (deepest sample taken at 4710 m) of the GEOSECS cruise (1978) located near the OISO-ST11 sampling site (405 and 465 km away from it, respectively; Fig. 1). All the reoccupations used in this analysis are listed in Table 1. Since seasonal variations are only observed in the surface mixed layer (Metzl et al., 2006), we used the observations available for all seasons (Table 1).

3.2 Validation of the data

For 1998–2004, the OISO data were quality-controlled in CARINA (Lo Monaco et al., 2010) and for 2005 and 2009–2011 in GLODAPv2 (Key et al., 2015; Olsen et al.,

Table 1. List of the cruises used in this study.

Cruise	Station	Location	Year	Month
GEOSECS	430	61.0° E, 60.0° S	1978	February
INDIGO-1	14	58.9° E, 53.0° S	1985	March
INDIGO-3	75	63.2° E, 56.5° S	1987	January
OISO-01	11	63.0° E, 56.5° S	1998	February
OISO-03	11	63.0° E, 56.5° S	1998	December
OISO-05	11	63.0° E, 56.5° S	2000	August
OISO-06	11	63.0° E, 56.5° S	2001	January
OISO-08	11	63.0° E, 56.5° S	2002	January
OISO-11	11	63.0° E, 56.5° S	2004	January
OISO-18	11	63.0° E, 56.5° S	2009	December
OISO-19	11	63.0° E, 56.5° S	2011	January
OISO-21	11	63.0° E, 56.5° S	2012	February
OISO-23	11	63.0° E, 56.5° S	2014	January
OISO-26	11	63.0° E, 56.5° S	2016	October
OISO-27	11	63.0° E, 56.5° S	2017	January
OISO-28	11	63.0° E, 56.5° S	2018	January

2016, 2019). The three additional datasets from GEOSECS, INDIGO-1 and INDIGO-3 were first qualified in GLODAPv1 (Key et al., 2004) and used for the first C_{ant} estimates in the Indian Ocean (Sabine et al., 1999). The adjustments recommended for these historical datasets have been revisited in CARINA and GLODAPv2. In this paper we used the revised adjustments applied to the GLODAPv2 data product, with one exception for the total alkalinity (A_T) data from INDIGO-3 for which we applied an intermediate adjustment between the recommendation from GLODAPv1 (confirmed in CARINA) for no adjustment (due to a lack of available observations in this region for robust comparison) and the adjustment by $-8 \mu\text{mol kg}^{-1}$ applied to the GLODAPv2 data product (justification in the Supplement).

For the recent OISO cruises conducted in 2012–2018 not yet included in the most recent GLODAPv2 product, we have proceeded to a data quality control in deep water in which C_{ant} concentrations are low and subject to very small changes from year to year (see the Supplement).

3.3 Biogeochemical measurements

Measurement methods during OISO cruises were previously described (Jabaud-Jan et al., 2004; Metzl et al., 2006). In short, measurements were obtained using conductivity–temperature–depth (CTD) casts fixed on a 24 bottles rosette equipped with 12 L General Oceanics Niskin bottles. Potential temperature (Θ) and salinity (S) measurements have an accuracy of 0.002 °C and 0.005, respectively. A_T and C_T were sampled in 500 mL glass bottles and poisoned with 100 μL of mercuric chloride saturated solution to halt biological activity. Discrete C_T and A_T samples were analyzed onboard by potentiometric titration derived from the method developed by Edmond (1970) using a closed cell. The repeatability for C_T and A_T varies from 1 to $3.5 \mu\text{mol kg}^{-1}$

(depending on the cruise) and is determined by sample duplicates (at the surface, at 1000 m and in bottom water). The accuracy of C_T and A_T measurements (always better than $\pm 3 \mu\text{mol kg}^{-1}$ for all cruises since 1998) was ensured by daily analyses of Certified Reference Materials (CRMs) provided by the A.G. Dickson laboratory (Scripps Institute of Oceanography). The dissolved oxygen (O_2) concentration was determined by an oxygen sensor fixed on the rosette. These values were adjusted using measurements obtained by Winkler titrations using a potentiometric titration system (at least 12 measurements for each profile). The thiosulfate solution used for the Winkler titration was calibrated using iodate standard solution (provided by Ocean Scientific International Limited) to ensure the standard O_2 accuracy of $2 \mu\text{mol kg}^{-1}$. Nitrate (NO_3) and silicate (Si) concentrations were measured onboard or onshore with an automatic colorimetric Technicon analyzer following the methods described by Tréguer and Le Corre (1975) until 2008 and the revised protocol described by Coverly et al. (2009) since 2009. Based on replicate measurements for deep samples we estimate an error of about 0.3 % for both nutrients. NO_3 data are not available for all the cruises used in this analysis. The mean NO_3 concentration in the LAABW at OISO-ST11 is $32.8 \pm 1.2 \mu\text{mol kg}^{-1}$, while the average value derived from the GLODAP-v2 database in bottom water south of 50° S in the southern Indian Ocean is $32.4 \pm 0.6 \mu\text{mol kg}^{-1}$. The lack of NO_3 data for few cruises has been palliated by using a climatological value of $32.4 \mu\text{mol kg}^{-1}$ with a limited impact on C_{ant} determined by the C° method ($< 2 \mu\text{mol kg}^{-1}$ for estimates based on the differences observed between NO_3 measurements and the climatological value).

3.4 C_{ant} calculation using the TrOCA method

The TrOCA method was first presented by Touratier and Goyet (2004a, b) and revised by Touratier et al. (2007). Following the concept of the quasi-conservative tracer NO (Broecker, 1974), TrOCA is a tracer defined as a combination of O_2 , C_T and A_T following

$$\text{TrOCA} = O_2 + a \left(C_T - \frac{1}{2} A_T \right), \quad (1)$$

where a is defined in Touratier et al. (2007) as a combination of the Redfield equation coefficients for CO_2 , O_2 , HPO_4^{2-} and H^+ . For more details about the definition and the calibration of this parameter, please refer to Touratier et al. (2007). The temporal change in TrOCA is independent of biological processes and can be attributed to anthropogenic carbon (Touratier and Goyet, 2004a). Therefore, C_{ant} can be directly calculated from the difference between TrOCA and its preindustrial value TrOCA^0 :

$$C_{\text{ant}} = \frac{\text{TrOCA} - \text{TrOCA}^0}{a}, \quad (2)$$

where TrOCA⁰ is evaluated as a function of Θ and A_T (Eq. 3) as

$$\text{TrOCA}^0 = e^{\left[b - (c)\Theta - \frac{d}{A_T^2} \right]} \quad (3)$$

In these expressions, the coefficients a , b , c and d were adjusted by Touratier et al. (2007) from deep water free of anthropogenic CO₂ using the tracers $\Delta^{14}\text{C}$ and CFC-11 from the GLODAPv1 database (Key et al., 2004). The final expression used to calculate C_{ant} is

$$C_{\text{ant}} = \frac{\text{O}_2 + 1.279 \left(C_T - \frac{1}{2} A_T \right) - e^{\left[7.511 - (1.087 \cdot 10^{-2})\Theta - \frac{7.81 \cdot 10^5}{A_T^2} \right]}}{1.279} \quad (4)$$

The consideration of the errors on the different parameters involved in the TrOCA method results in an uncertainty of $\pm 6.25 \mu\text{mol kg}^{-1}$ (mostly due to the parameter a , leading to $\pm 3.31 \mu\text{mol kg}^{-1}$). As this error is relatively large compared to the expected C_{ant} concentrations in deep and bottom SO water (Pardo et al., 2014) we will compare the TrOCA results using another indirect method to interpret C_{ant} changes over 40 years.

3.5 C_{ant} calculation using the preformed inorganic carbon (C^0) method

To support the C_{ant} trend determined with the TrOCA method, C_{ant} was also estimated using a back-calculation approach denoted C^0 (Brewer, 1978; Chen and Millero, 1979), previously adapted for C_{ant} estimates along the WOCE-I6 section between South Africa and Antarctica (Lo Monaco et al., 2005a). This method consists of the correction of the measured C_T for the biological contribution (C_{bio}) and preindustrial preformed C_T (C_{PI}^0):

$$C_{\text{ant}} = C_T - C_{\text{bio}} - C_{\text{PI}}^0 \quad (5)$$

C_{bio} (Eq. 6) depends on carbonate dissolution and organic matter remineralization, taking account of the corrected C/O_2 ratio from Körtzinger et al. (2001):

$$C_{\text{bio}} = 0.5 \Delta A_T - (C/\text{O}_2 + 0.5 N/\text{O}_2) \Delta \text{O}_2, \quad (6)$$

where $C/\text{O}_2 = 106/138$ and $N/\text{O}_2 = 16/138$. ΔA_T and ΔO_2 are the difference between the measured values (A_T and O_2) and the preformed values (A_T^0 and O_2^0). A_T^0 (Eq. 7) has been computed by Lo Monaco et al. (2005a) as a function of Θ , S and the conservative tracer PO:

$$A_T^0 = 0.0685 \text{PO} + 59.79 S - 1.45 \Theta + 217.1. \quad (7)$$

PO (Eq. 8) has been defined by Broecker (1974) and depends on the equilibrium of O_2 with phosphate (PO_4). When PO_4 data are not available, nitrate (NO_3) can be used instead as follows (the N/P ratio of 16 is from Anderson and Sarmiento, 1994):

$$\text{PO} = \text{O}_2 + 170 \text{PO}_4 = \text{O}_2 + (170/16) \text{NO}_3. \quad (8)$$

To determine O_2^0 , it is assumed that the surface water is in full equilibrium with the atmosphere ($\text{O}_2^0 = \text{O}_{2,\text{sat}}$; Benson and Krause, 1980) and that after subduction O_2 in a given water mass is only impacted by the biological activity (Weiss, 1970). A correction of O_2^0 has been proposed by Lo Monaco et al. (2005a) to take account of the undersaturation of O_2 due to sea ice cover at high latitudes. O_2^0 is therefore corrected by assuming a mean mixing ratio of the ice-covered surface water $k = 50\%$ (Lo Monaco et al., 2005a) and a mean value for O_2 undersaturation in ice-covered surface water $\alpha = 12\%$ (Anderson et al., 1991) according to Eq. (9):

$$\Delta \text{O}_2 = (1 - \alpha k) \text{O}_{2,\text{sat}} - \text{O}_2 = \text{AOU}. \quad (9)$$

C_{PI}^0 in Eq. (5) is a function of the current preformed C_T (C_{obs}^0) and a reference water term (Eq. 10):

$$C_{\text{PI}}^0 = C_{\text{obs}}^0 + \left[C_T - C_{\text{bio}} - C_{\text{obs}}^0 \right]_{\text{REF}}. \quad (10)$$

C_{obs}^0 has been computed similarly as A_T^0 (Eq. 11):

$$C_{\text{obs}}^0 = -0.0439 \text{PO} + 42.79 S - 12.02 \Theta + 739.8, \quad (11)$$

where the reference water term is a constant for a given time of observation corresponding to the time when C_{obs}^0 is parameterized. In this paper, we used the parameterization given by Lo Monaco et al. (2005a) and their estimated value for the reference term of $51 \mu\text{mol kg}^{-1}$. This number has been computed using an optimum multiparametric (OMP) model to estimate the mixing ratio of the North Atlantic deep water in the SO (used as reference water, i.e., old water mass, where $C_{\text{ant}} = 0$). For more details about the C^0 method, which has a final error of $\pm 6 \mu\text{mol kg}^{-1}$, please see Lo Monaco et al. (2005a).

4 Results

The vertical distribution of hydrological and biogeochemical properties observed in deep and bottom water and their evolution over the last 40 years are displayed in Fig. 2. The LCDW layer ($\gamma^n = 28.15\text{--}28.27 \text{ kg m}^{-3}$) is characterized by minimum O_2 concentrations (Fig. 2c), higher C_T (Fig. 2b) and lower C_{ant} concentrations than the AABW (Fig. 2a). C_{ant} concentrations were not significant in the LCDW until the end of the 1990s ($< 6 \mu\text{mol kg}^{-1}$); then our data show an increase in C_{ant} between the two 1998 reoccupations, followed by relatively constant C_{ant} concentrations ($10 \pm 3 \mu\text{mol kg}^{-1}$). In the LAABW ($\gamma^n > 28.35 \text{ kg m}^{-3}$), well identified by low Θ , low S and high O_2 , C_{ant} concentrations are higher than in the overlying UAABW and LCDW (Fig. 2a). The evolutions of the mean properties in the LAABW over 40 years are shown in Fig. 3. In this layer, C_{ant} concentrations increased from $5 \pm 4 \mu\text{mol kg}^{-1}$ in 1978 and $7 \pm 4 \mu\text{mol kg}^{-1}$ in the mid-1980s to $13 \pm 2 \mu\text{mol kg}^{-1}$ at the end of the 1990s and up to $19 \pm 2 \mu\text{mol kg}^{-1}$ in 2004

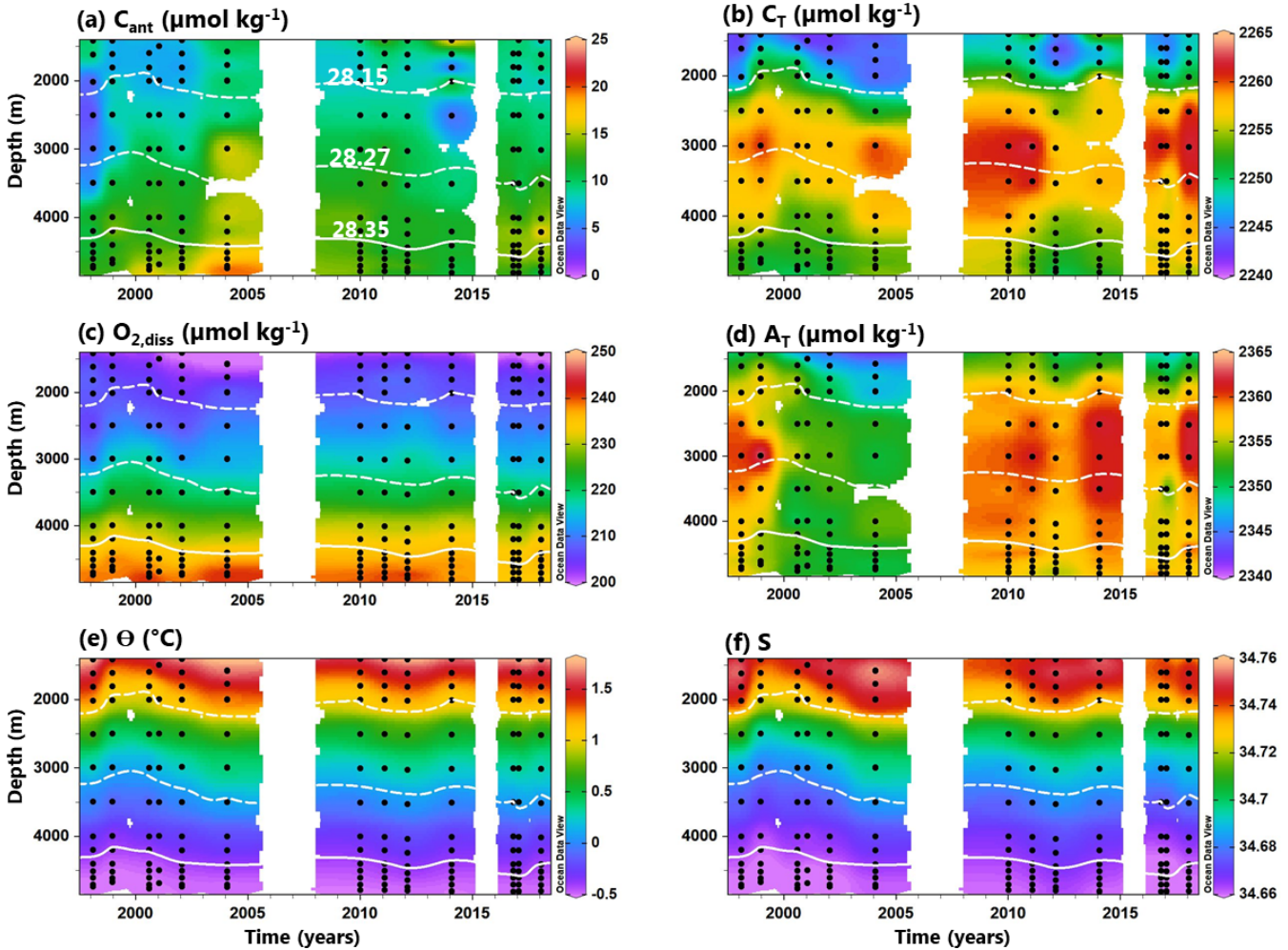


Figure 2. Hovmöller diagram of (a) C_{ant} via TrOCA, (b) C_T , (c) O_2 , (d) A_T , (e) Θ and (f) S based on the OISO data presented in Table 1. Data points are represented by black dots. The white isolines represent the water mass separation by γ^n (from the bottom: LAABW, UAABW and LCDW). Figure produced with Ocean Data View (Schlitzer, 2019).

(Fig. 3a). Figure 3a also shows a very good agreement between the TrOCA method and the C^0 method for both the magnitude and variability of C_{ant} in the LAABW. Our results show a mean C_{ant} trend in the LAABW of $+1.4 \mu\text{mol kg}^{-1}$ per decade over the full period and a maximum trend of the order of $+5.2 \mu\text{mol kg}^{-1}$ per decade over 1987–2004 (Table 2). Due to the mixing of AABW with old LCDW (C_{ant} free), these trends are lower than the theoretical trend expected from the increase in atmospheric CO₂. Indeed, assuming that the surface ocean $f\text{CO}_2$ follows the atmospheric growth rate ($+1.8 \text{atm yr}^{-1}$ over 1978–2018) in the seasonal ice zone (Roden et al., 2016), the theoretical C_{ant} trend at AABW formation sites would be of the order of $+8 \mu\text{mol kg}^{-1}$ per decade in the Antarctic surface water. This is close to the theoretical C_T trend estimated for freezing shelf water in the Weddell Sea (van Heuven et al., 2014).

Over the full period, C_T increased by $2.0 \pm 0.5 \mu\text{mol kg}^{-1}$ per decade, mostly due to the accumulation of C_{ant} (Table 2).

Our data also show a significant decrease in O_2 concentrations by $0.8 \pm 0.4 \mu\text{mol kg}^{-1}$ per decade over the 40-year period (Fig. 3c, Table 2) that could be caused by reduced ventilation, as suggested by Schmidtko et al. (2017), who observed significant O_2 loss in the global ocean. In the deep Indian SO sector, these authors found a trend approaching $-1 \mu\text{mol kg}^{-1}$ per decade over 50 years (1960–2010), which is consistent with our data. We did not detect any significant trend in A_T , Θ and S over the full period, but over shorter periods our data show a significant decrease in A_T . The low A_T values observed over 2000–2004 (Fig. 3d) could suggest reduced calcification in the upper ocean, leading to less sinking of calcium carbonate tests and a decrease in A_T in deep and bottom water over this period (Fig. 2d). For this period the increase in C_T was lower than the accumulation of C_{ant} , but such a feature is disputable in view of the uncertainty on the C_{ant} calculation. This event is followed by an increase in the “natural” component of C_T (C_{nat} , calculated as the difference

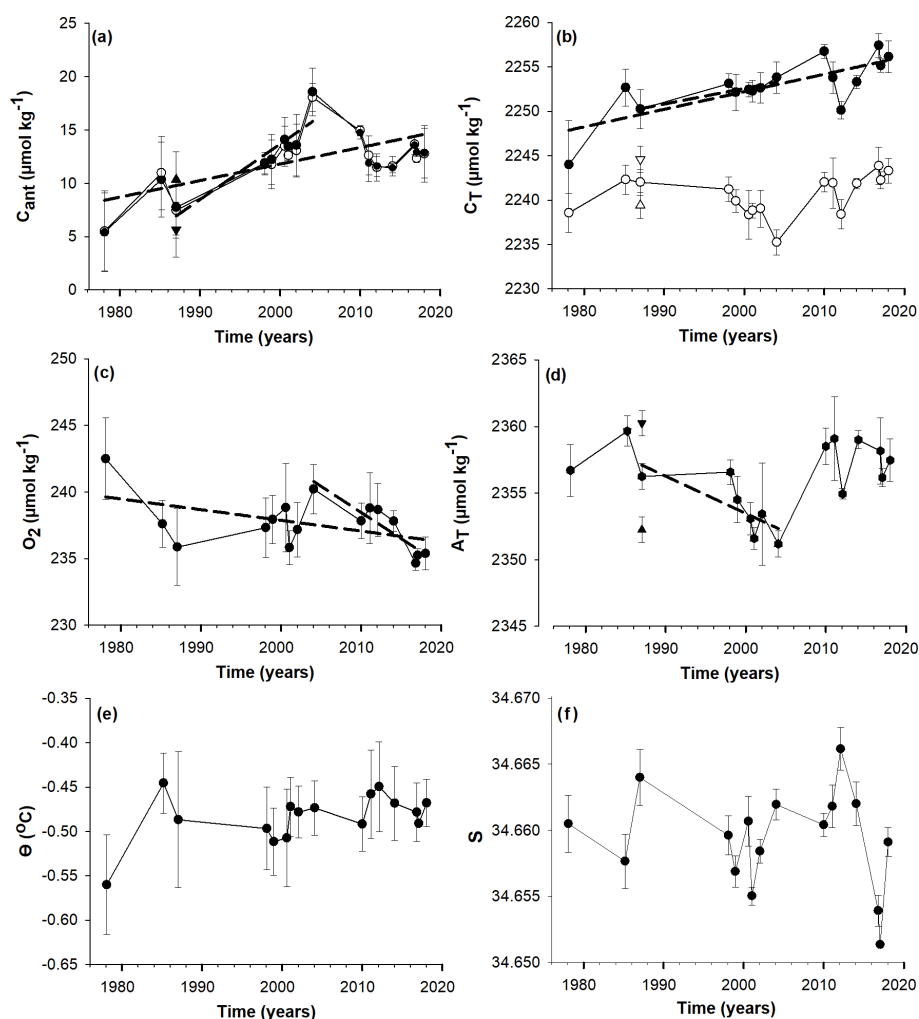


Figure 3. Interannual variability (dashed lines) and significant trends (at 95 %, see Table 2; dotted lines) for the 40 years of observation of the OISO-ST11 LAABW properties, including (a) C_{ant} by the TrOCA (black circles and triangles) and the C^0 (open circles) method, (b) C_T (black circles) and C_{nat} (open circles), (c) O_2 , (d) A_T , (e) Θ , and (f) S . For (a) C_{ant} , (b) C_{nat} and (d) A_T , the triangles pointing up and down correspond to INDIGO-3 values with and without $-8 \mu\text{mol kg}^{-1}$ of correction on the A_T , respectively (see the Supplement for more details).

Table 2. Trends (per decade) of observed and calculated properties in the LAABW estimated over different periods (in bold: significant trends at the 95 % confidence level).

Period	S	Θ °C	Si $\mu\text{mol kg}^{-1}$	NO_3 $\mu\text{mol kg}^{-1}$	O_2 $\mu\text{mol kg}^{-1}$	A_T $\mu\text{mol kg}^{-1}$	C_T $\mu\text{mol kg}^{-1}$	C_{ant} TrOCA $\mu\text{mol kg}^{-1}$
1978–2018	-0.001 ± 0.001	0.01 ± 0.01	-1.2 ± 0.9	0.2 ± 0.2	-0.8 ± 0.4	-0.1 ± 0.1	2.0 ± 0.5	1.4 ± 0.5
1987–2018	-0.001 ± 0.001	0.01 ± 0.01	-1.9 ± 1.4	0.3 ± 0.4	-0.3 ± 0.5	0.6 ± 0.1	1.6 ± 0.5	1.1 ± 0.8
1987–2004	-0.003 ± 0.002	0.01 ± 0.01	-6.5 ± 1.8	0.9 ± 0.9	1.7 ± 1.0	-1.9 ± 1.1	1.8 ± 0.4	5.2 ± 1.1
2004–2018	-0.006 ± 0.003	0.01 ± 0.01	-1.8 ± 4.5	-0.5 ± 1.0	-3.9 ± 0.7	3.4 ± 0.2	1.7 ± 1.9	-3.5 ± 1.5

between C_T and C_{ant}) since 2004 associated with a decrease in O_2 and no increase in C_{ant} (Table 2). These trends were not associated with a significant trend in Θ or S (Fig. 3e, f, Table 2). The increase in C_{nat} is thus unlikely to originate from increased mixing with LCDW during bottom water transport, confirming that our LAABW definition excludes mixing with

the LCDW. Enhanced organic matter remineralization is also unlikely since NO_3 did not show any significant trend (Table 2).

Importantly, our data show substantial interannual variations in LAABW properties, which could significantly impact the trends estimated from limited reoccupations (e.g.,

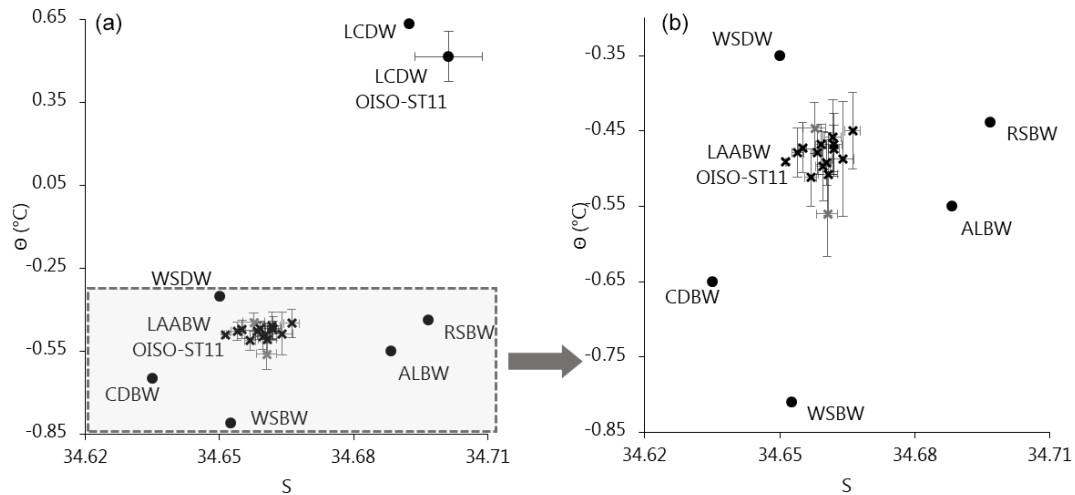


Figure 4. (a) Full Θ – S diagram of studied water masses and (b) a zoom-in to bottom water. Values are from the literature for the WSBW (Fukamachi et al., 2010; van Heuven, 2013; Pardo et al., 2014; Robertson et al., 2002), the WSDW (Carmack and Foster, 1975; Fahrback et al., 1994; van Heuven, 2013; Robertson et al., 2002), the RSBW (Fukamachi et al., 2010; Johnson, 2008; Pardo et al., 2014), the ALBW (Fukamachi et al., 2010; Johnson, 2008; Pardo et al., 2014), the CDBW (Ohshima et al., 2013) and the LCDW (Lo Monaco et al., 2005a; Pardo et al., 2014; Smith and Treguer, 1994), as well as from the OISO-ST11 dataset for the OISO-ST11 LAABW and OISO-ST11 LCDW. Error bars are calculated from the individual annual averaged values for the OISO-ST11 LAABW and from all data for the OISO-ST11 LCDW. For the OISO-ST11 LAABW, the grey cross are the GEOSECS (lowest Θ) and INDIGO-1 (highest Θ) values.

Williams et al., 2015; Pardo et al., 2017; Murata et al., 2019). For example, we found relatively higher C_{ant} concentrations in 1985 ($10 \mu\text{mol kg}^{-1}$) compared to 1978 ($5 \mu\text{mol kg}^{-1}$) and 1987 ($7 \mu\text{mol kg}^{-1}$). This is linked to a signal of low S in 1985 (Fig. 3f) that could be due to a larger contribution of fresher water such as the WSDW or CDBW. This could also be related to the different sampling locations. Over the last decade (2009–2018), our data show large and rapid changes in S that are partly reflected in C_T and O_2 and that could explain the relatively low C_{ant} concentrations observed over this period. Indeed, the S maximum observed in 2012 (correlated to higher Θ) is associated with a marked C_T minimum (surprisingly almost as low as in 1987), as well as low A_T (hence low C_{nat}) and low NO_3 concentrations. Since these anomalies were associated with a decrease in C_{ant} concentrations, one may argue for an increased contribution of bottom water ventilated far away from our study site. A few years later our data show an S minimum (correlated with lower Θ) associated with a rapid increase in C_T and a rapid decrease in O_2 between 2013 and 2016, suggesting the contribution of a closer AABW type such as the CDBW. The freshening of -0.006 per decade in S between 2004 and 2018 that we observed on the western side of the Kerguelen Plateau was also observed on the eastern side of the plateau by Menezes et al. (2017) over a similar period. In this region, Menezes et al. (2017) evaluated a change in S by about -0.008 per decade from 2007 to 2016 (against -0.002 per decade between 1994 and 2007), suggesting an acceleration of AABW freshening in recent years. However, they also reported a warming by $+0.06$ °C per decade, while we observed cooler

temperatures in 2016–2018. This suggests that we sampled a different mixture of AABW.

5 Discussion

5.1 LAABW composition at OISO-ST11

At each formation site, AABW experiences significant temporal property changes, mostly recognized at a decadal scale (e.g., freshening in the southern Indian Ocean; Menezes et al., 2017), with a potential impact on carbon uptake and C_{ant} concentrations during AABW formation (Shadwick et al., 2013). The Θ – S diagram constructed from yearly averaged data in bottom water (Fig. 4) shows that the LAABW at OISO-ST11 is a complex mixture of WSDW, CDBW, RSBW and ALBW. The coldest type of LAABW was observed at the GEOSECS station at 60° S (-0.56 °C), while the warmer type of LAABW was observed at the INDIGO-1 station at 53° S (-0.44 °C). These extreme Θ values could be a natural feature or may be related to specific sampling. For the other cruises, Θ in LAABW ranges from -0.51 to -0.45 °C with no clear indication of the specific AABW origin. The S range observed in the bottom water at OISO-ST11 (34.65 – 34.67) illustrates either changes in mixing with various AABW sources or temporal variations at the formation site. Given knowledge of deep and bottom water circulation and characteristics (Figs. 1 and 4) and the significant C_{ant} concentrations that we calculated in the LAABW (Fig. 3a), the main contribution at our location is likely the younger and colder CDBW for which relatively high C_{ant} concentrations

have been recently documented (Roden et al., 2016). From its formation region, the CDBW can either flow westward with the CAC or flow northward in the Enderby Basin (Ohshima et al., 2013; Fig. 1). In the CAC branch, the CDBW mixes with the LCDW along the Antarctic shelf and the continental slope between 80 and 30° E (Meijers et al., 2010; Roden et al., 2016). On the western side of the Kerguelen Plateau, CDBW also mixes with RSBW and ALBW (Orsi et al., 1999; Van Wijk and Rintoul, 2014). In this context, the C_{ant} concentrations observed in the bottom layer at OISO-ST11 are probably not linked to one single AABW source but are likely a complex interplay of AABW from different sources with different biogeochemical properties.

5.2 C_{ant} concentrations

In order to compare our C_{ant} estimates with other studies, we separated the 40-year time series into three periods: the first period (1978–1987) corresponds to historical data when C_{ant} is expected to be low; the second period (1998–2004) starts when the first OISO cruise was conducted (using CRM for A_{T} and C_{T} measurements) and ends when C_{ant} concentrations in the LAABW are maximum (Fig. 3a); and the third period consists of the observations performed in late 2009 to 2018 when the observed variations are relatively large for S and small for C_{ant} . The mean C_{ant} concentrations for each period are 7, 14 and 13 $\mu\text{mol kg}^{-1}$, respectively, which is consistent with the results from other studies (Table 3). The C_{ant} values for 1978–1987 can hardly be compared to other studies because very few observations were conducted in the 1980s in the Indian sector of the SO (Sabine et al., 1999) and because of potential biases for historical data despite their careful quality control in GLODAP and CARINA (Key et al., 2004; Lo Monaco et al., 2010; Olsen et al., 2016). In addition, the different methods used to estimate C_{ant} can lead to different results, especially in deep and bottom water of the SO (Vázquez-Rodríguez et al., 2009). Overall, Table 3 confirms that C_{ant} concentrations were low in the 1970s and 1980s and reached values of the order of 10 $\mu\text{mol kg}^{-1}$ in the 1990s, a signal not clearly captured in global data-based estimates (Gruber, 1998; Sabine et al., 2004; Waugh et al., 2006; Khatiwala et al., 2013).

The observations presented in this analysis, although regional, offer a complement to recent estimates of C_{ant} changes evaluated between 1994 and 2007 in the top 3000 m for the global ocean (Gruber et al., 2019a). In the Enderby Basin at the horizon at 2000–3000 m, the accumulation of C_{ant} from 1994 to 2007 is not uniform and ranges between 0 and 8 $\mu\text{mol kg}^{-1}$ (Gruber et al., 2019a). At our station, in the LCDW (2000–3000 m) the C_{ant} concentrations were not significant in 1978–1987 (-2 to 5 $\mu\text{mol kg}^{-1}$) but increase to an average of 9 ± 3 $\mu\text{mol kg}^{-1}$ in 1998–2018 (Fig. 2a), probably due to mixing with AABW that contains more C_{ant} . Interestingly, this value is close but in the high range of the C_{ant}

accumulation estimated from 1994 to 2007 in deep water of the southern Indian Ocean (Gruber et al., 2019a).

Not surprisingly, high C_{ant} concentrations are detected in the AABW formation regions (Table 3). The highest C_{ant} concentrations in bottom water (up to 30 $\mu\text{mol kg}^{-1}$) were observed in the ventilated shelf water in the Ross Sea (Sandrini et al., 2007). In the Adélie and Mertz polynya regions, Shadwick et al. (2014) observed high C_{ant} concentrations in the subsurface shelf water (40–44 $\mu\text{mol kg}^{-1}$) but lower values in the ALBW (15 $\mu\text{mol kg}^{-1}$) due to mixing with older LCDW. In WSBW, all C_{ant} concentrations estimated from observations between 1996 and 2005 and with the TrOCA method (Table 3) lead to about the same values ranging between 13 and 16 $\mu\text{mol kg}^{-1}$ (Lo Monaco et al., 2005b; van Heuven et al., 2011). In bottom water formed near Cape Darnley (CDBW), Roden et al. (2016) estimated high C_{ant} concentrations in bottom water (25 $\mu\text{mol kg}^{-1}$) resulting from the shelf water that contains very high amounts of C_{ant} (50 $\mu\text{mol kg}^{-1}$). The comparison with other studies confirms that far from the AABW formation sites, contemporary C_{ant} concentrations do not exceed 16 $\mu\text{mol kg}^{-1}$ on average.

5.3 C_{ant} trends and variability

Comparison of long-term C_{ant} trends in deep and bottom water of the SO is limited to very few regions where repeated observations are available. To our knowledge, only three other studies have evaluated the long-term C_{ant} trends in the SO based on more than five reoccupations: in the southwestern Atlantic (Ríos et al., 2012) and in the Weddell gyre along the prime meridian section (van Heuven et al., 2011, 2014). Temporal changes in C_{T} and C_{ant} have also been investigated in other SO regions but limited to two to four reoccupations (Williams et al., 2015; Pardo et al., 2017; Murata et al., 2019). Given the C_{ant} variability depicted at our location (Fig. 3a), different trends can be deduced from limited reoccupations. As an example, Murata et al. (2019) evaluated the change in C_{ant} from data collected 17 years apart (1994–1996 and 2012–2013) along a transect around 62° S and found a small increase at our location (<5 $\mu\text{mol kg}^{-1}$ around 60° E). This result appears very sensitive to the time of the observation given that we found a minimum in C_{ant} concentrations between 2011 and 2014 (Fig. 3a) associated with a marked C_{T} minimum (Fig. 3b). In addition, our results show that the detection of C_{ant} trends appears very sensitive to the time period considered (Table 2). As an extreme case, the C_{ant} trend calculated for the period 1987–2004 is +5.2 $\mu\text{mol kg}^{-1}$ per decade (relatively close to the theoretical C_{ant} trend of +8 $\mu\text{mol kg}^{-1}$ per decade), but it reverses to -3.5 $\mu\text{mol kg}^{-1}$ per decade for the period 2004–2018.

The long-term C_{T} trend that we estimated in the LAABW in the eastern Enderby Basin (2.0 ± 0.5 $\mu\text{mol kg}^{-1}$ per decade) is slightly faster than the C_{T} trends estimated in the WSBW in the Weddell gyre:

Table 3. Compilation of C_{ant} sequestration investigations in the AABW ($\gamma^{\text{tr}} \geq 28.25 \text{ kg m}^{-3}$) using the TrOCA method. The C_{ant} estimation of Pardo et al. (2014) is calculated using theoretical AABW mean composition (with 3 % of ALBW) and the carbon data from the GLODAPv1 and CARINA databases. Sandrini et al. (2007) values have been measured at the bottom of the Ross Sea and correspond to recently sinking high-salinity shelf water (HSSW). The mean values published by Roden et al. (2016) for the AABW present WSDW characteristics but can be a mix of CDBW and LCDW.

Source	Location	Water masses considered	Year	C_{ant} ($\mu\text{mol kg}^{-1}$)
Pardo et al. (2014) Fig. 5	Averaged AABW composition	WSBW–RSBW–ALBW	1994	12
Lo Monaco et al. (2005b) Fig. 4b	WOCE line I6 (30° E; 50–70° S)	WSBW CDBW	1996	15 20
Sandrini et al. (2007) Fig. 4a	Ross Sea	HSSW (previous RSBW)	2002/2003	Max. of 30
Shadwick et al. (2014) Table 2	Mertz polynya and Adélie depression	ALBW	2007/2008	15
Roden et al. (2016) Table 2	Southern Indian Ocean (30–80° E; 60–69° S)	WSDW–LCDW–CDBW	2006	25
van Heuven et al. (2011) Fig. 13	Weddell gyre (0° E; 55–71° S)	WSBW	2005	16
This study	Enderby Basin (56.5° S, 63° E)	LAABW	1978–1987	8 ± 3
		(mix of WSDW–CDBW–RSBW–ALBW)	1987–1998	10 ± 4
			1987–2004	13 ± 4
			1998–2004	14 ± 2
			2010–2018	13 ± 1
		1978–2018	12 ± 3	

+1.2 ± 0.5 $\mu\text{mol kg}^{-1}$ per decade over the period 1973–2011 and +1.6 ± 1.4 $\mu\text{mol kg}^{-1}$ per decade when restricted to 1996–2011 (van Heuven et al., 2014). Along the SR03 line (south of Tasmania) reoccupied in 1995, 2001, 2008 and 2011, Pardo et al. (2017) calculated a C_{T} trend of +2.4 ± 0.2 $\mu\text{mol kg}^{-1}$ per decade in the AABW, composed of ALBW and RSBW in this sector. This is higher than the C_{T} trends found at our location and in the Weddell gyre, but surprisingly, this was not associated with a significant increase in C_{ant} . The C_{T} trend in AABW along the SR03 section was likely due to the intrusion of old and C_{T} -rich water also revealed by an increase in Si concentrations during 1995–2011 (Pardo et al., 2017). This is a clear example of decoupling between C_{T} and C_{ant} trends in deep and bottom water as observed at our location in the last decade (Table 2). For C_{ant} , our 40-year trend estimate (1.4 ± 0.5 $\mu\text{mol kg}^{-1}$ per decade) appears close to the trend reported by Ríos et al. (2012) in the southwestern Atlantic AABW from six reoccupations between 1972 and 2003 (+1.5 $\mu\text{mol kg}^{-1}$ per decade). However, if we limit our result to the period 1978–2002 or 1978–2004 (about the same period as in Ríos et al., 2012), our trend is much larger (+3–4 $\mu\text{mol kg}^{-1}$ per decade).

At our location, the C_{ant} trend over 40 years (+1.4 ± 0.5 $\mu\text{mol kg}^{-1}$ per decade) explains most of

the observed C_{T} increase (+2.0 ± 0.5 $\mu\text{mol kg}^{-1}$ per decade). The residual of +0.4 $\mu\text{mol kg}^{-1}$ per decade reflects changes in natural processes affecting the carbon content (different AABW sources, ventilation, mixing with deep water, remineralization or carbonates dissolution). Although this is a weak signal, the natural C_{T} change (C_{nat}) mirrors the observed decrease in O₂ by −0.8 ± 0.4 $\mu\text{mol kg}^{-1}$ per decade. This O₂ decrease detected in the Enderby Basin appears to be a real feature that was documented at a large scale for 1960–2010 in deep SO basins (Schmidtko et al., 2017), suggesting that the changes observed at 63° E, 56.5° S are related to large-scale processes, possibly due to a decrease in AABW formation (Purkey and Johnson, 2012).

5.4 Recent C_{ant} stability

Although most studies suggest a gradual accumulation of C_{ant} in the AABW, our time series highlights significant multi-annual changes, in particular over the last decade when C_{ant} concentrations were as low as around the year 2000 (Fig. 3a) and decoupled from the increase in C_{T} (Fig. 3b). This result is difficult to interpret because at our location, away from AABW sources (Fig. 1), the temporal variability observed in the LAABW layer can result from many remote processes occurring at the AABW formation sites

(such as wind forcing, ventilation, sea ice melting, thermodynamic, biological activity and air–sea exchanges). Additionally, internal processes during the transport of AABW (such as organic matter remineralization, carbonate dissolution and mixing with surrounding water) must also be taken into account. The apparent steady C_{ant} feature suggests that AABW found at our location has stored less C_{ant} in recent years. This might be linked to reduced CO₂ uptake in the AABW formation regions, as recognized at a large scale in the SO from the late 1980s to 2001 (Le Quéré et al., 2007; Metzl, 2009; Lenton et al., 2012; Landschützer et al., 2015). This large-scale response in the SO during a positive trend in the Southern Annular Mode (SAM) is mainly associated with stronger winds driven by accelerating greenhouse gas emissions and stratospheric ozone depletion, leading to warming and freshening in the SO (Swart et al., 2018), a change in the ventilation of C_{T} -rich deep water, and reduced CO₂ uptake (Lenton et al., 2009). The reconstructed $p\text{CO}_2$ fields by Landschützer et al. (2015) suggest that the reduced CO₂ sink in the 1990s is identified at high latitudes in the SO (see Figs. 2a and S9 in Landschützer et al., 2015). However, as opposed to the circumpolar open ocean zone (e.g., Metzl, 2009; Takahashi et al., 2009, 2012; Munro et al., 2015; Fay et al., 2018), the long-term trend of surface $f\text{CO}_2$ and carbon uptake deduced from direct observations is not clearly identified in the seasonal ice zone (SIZ), the shelves around Antarctica, and thus in the AABW formation regions of interest to interpret our results (Laruelle et al., 2018). There, surface $f\text{CO}_2$ data are sparse, especially before 1990, and cruises were mainly conducted in austral summer when the spatiotemporal $f\text{CO}_2$ variability is very large and driven by multiple processes at regional or small scales, such as primary production, sea ice formation and retreat, and water circulation and mixing. This leads to various estimates of the air–sea CO₂ fluxes around Antarctica depending on the region and period and large uncertainty when attempting to detect long-term trends (Gregor et al., 2018).

In particular, in polynyas and AABW formation regions where $f\text{CO}_2$ is low and where katabatic winds prevail, a very strong instantaneous CO₂ sink can occur at the local scale (up to $-250 \text{ mmol C m}^{-2} \text{ d}^{-1}$ in Terra Nova Bay in the Ross Sea according to DeJong and Dunbar, 2017). In the Prydz Bay region where CDBW is formed, recent studies show that surface $f\text{CO}_2$ in austral summer varies over a very large range (150–450 μatm), with the lowest $f\text{CO}_2$ observed in the shelf region generating a very strong local CO₂ sink ($-221 \text{ mmol C m}^{-2} \text{ d}^{-1}$; Roden et al., 2016). The carbon uptake was particularly enhanced near Cape Darnley and coincided with the highest C_{ant} concentrations that Roden et al. (2016) estimated in the dense shelf water that subducts to form AABW. In the Prydz Bay coastal region, surface $f\text{CO}_2$ values in 1993–1995 were as low as 100 μatm (Gibson and Trull, 1999), leading to a strong local CO₂ uptake of $-30 \text{ mmol C m}^{-2} \text{ d}^{-1}$ in summer. In addition, Roden et al. (2013) found a large C_{T} increase over 16 years

($+34 \mu\text{mol kg}^{-1}$) in the Prydz Bay, which is much higher than the anthropogenic signal alone ($+12 \mu\text{mol kg}^{-1}$) and likely explained by changes in primary production that would have been stronger in 1994. To our knowledge, this is the only direct observation of decadal C_{T} change in surface water in a region of AABW formation (here the Prydz Bay), and it highlights the difficulty not only of evaluating the C_{T} and C_{ant} long-term trends in these regions but also separating natural and anthropogenic signals when this water reaches the deep ocean. We attempted to detect long-term changes in CO₂ uptake in this region using the qualified $f\text{CO}_2$ data available in the SOCAT database (Bakker et al., 2016), but our estimates (not shown) were highly uncertain due to very large spatial and temporal variability. To conclude, all previous studies conducted near or in AABW formation sites clearly reveal that these regions are potentially strong carbon sinks, but how the sink changed over the last decades is not yet evaluated, and thus we are not able to certify that the recent C_{ant} stability that we observed in the LAABW at our location is directly linked to the weakening of the carbon sink that was recognized at the large scale in the SO from the 1980s to mid-2000s (Le Quéré et al., 2007; Landschützer et al., 2015).

Changes in the accumulation of C_{ant} in AABW could also be directly related to changes in physical processes occurring in AABW formation regions. Decadal decreasing of sea ice production and melting of sea ice have been documented in several regions, including Cape Darnley polynyas (Tamura et al., 2016; Williams et al., 2016). The consequent changes in Antarctic surface water properties are transmitted into the deep ocean, notably the well-recognized freshening of the AABW (Rintoul, 2007; Anilkumar et al., 2015). The warming of bottom water was also documented in the Enderby Basin (Couldrey et al., 2013) as well as at a larger scale in all deep SO basins (Purkey and Johnson, 2010; Desbruyères et al., 2016). Associated with a decrease in AABW formation in the 1990s (Purkey and Johnson, 2012), these physical changes could explain the recent stability of C_{ant} concentrations in AABW observed at our location. As AABW from different sources spreads and mixes with C_{T} -rich deep water before reaching our location (Fig. 1), less AABW formation and export would result in an increase in C_{T} (increase in C_{nat}) not associated with an increase in C_{ant} and a decrease in O₂ (as observed in recent years in Fig. 3a, b, c). Finally, it is also possible that the LAABW observed in recent years at our location is the result of a larger contribution of older RSBW, ALBW or even WSBW that has lower C_{ant} and O₂ concentrations compared to CDBW formed at Cape Darnley and Prydz Bay.

6 Conclusions

The distribution and evolution of C_{ant} in the bottom layer of the SO are related to complex interactions between cli-

matic forcing, air–sea CO₂ exchange at formation sites, and biological and physical processes during AABW circulation. The dataset that we collected regularly in the Enderby Basin over the last 20 years (1998–2018) in the framework of the OISO project, together with historical observations obtained in 1978, 1985 and 1987 (GEOSECS and INDIGO cruises), allows for the investigation of C_{ant} changes in AABW over 40 years in this region. The focus on AABW variability is made by defining Lower Antarctic Bottom Water (LAABW) as described in Sect. 2.3. Our results suggest that the accumulation of C_{ant} explains most, but not all, of the observed increase in C_{T} . We also detected a decrease in O₂ that is consistent with the large-scale signal reported by Schmidtko et al. (2017), possibly due to a decrease in AABW formation (Purkey and Johnson, 2012). Our data further indicate rapid anomalies in some periods, suggesting that for decadal to long-term estimates care has to be taken when analyzing the change in C_{ant} from datasets collected 10 or 20 years apart (e.g., Williams et al., 2015; Murata et al., 2019). Our results also show different C_{ant} trends over short periods, with a maximum increase of $5.2 \mu\text{mol kg}^{-1}$ per decade between 1987 and 2004 and apparent stability in the last 20 years (despite an increase in C_{T}). This suggests that AABW has stored less C_{ant} in the last decade, but our understanding of the processes that explain this signal is not clear. This might be the result of the reduced CO₂ uptake in the SO in the 1990s (Le Quéré et al., 2007; Landschützer et al., 2015), but this is not yet verified from direct C_{T} or $f\text{CO}_2$ observations in AABW formation regions due to the lack of winter data and very large variability during summer. This calls for more data collection and investigations in these regions. The apparent stability of C_{ant} in the LAABW since 1998 could also be directly linked to a decrease in AABW formation in the 1990s (Purkey and Johnson, 2012) or a change in the contributions of AABW from different sources, especially in the Prydz Bay region (Williams et al., 2016). In these scenarios, an increased contribution of C_{T} -rich and O₂-poor older LCDW along AABW transit would also explain the decoupling between C_{ant} and C_{T} (increase in C_{nat}) and decrease in O₂ concentrations observed in recent years, even if we tried to isolate this specific feature in our data selection. The decoupling between C_{ant} and C_{T} is not a unique feature, as it was also reported along the SR03 section between Tasmania and Antarctica, most probably due to advection of C_{T} -rich water (Pardo et al., 2017). This highlights the importance of the ocean circulation in influencing temporal C_{T} and C_{ant} inventory changes (De Vries et al., 2017) and the need to better separate anthropogenic and natural variability based on time series observations.

The evaluation and understanding of decadal C_{ant} changes in deep and bottom ocean water are still challenging, as the C_{ant} concentrations remain low compared to C_{T} measurement accuracy (at best $\pm 2 \mu\text{mol kg}^{-1}$, Bockmon and Dickson, 2015) and uncertainties of data-based methods ($\pm 6 \mu\text{mol kg}^{-1}$). Long-term repeated and qualified observa-

tions (at least 30 years) are needed to accurately detect and separate the anthropogenic signal from the internal ocean variability; we are thus only starting to document these trends that should now help to identify shortcomings in models regarding carbon storage in the deep SO (e.g., Frölicher et al., 2015). As changes in the SO (including warming, freshening, oxygenation and deoxygenation, CO₂, and acidification) are expected to accelerate in the future in response to anthropogenic forcing and climate change (e.g., Heuzé et al., 2015; Hauck et al., 2015; Ito et al., 2015; Yamamoto et al., 2015), it is important to maintain time series observations to complement the GO-SHIP strategy and to more regularly occupy other sectors of the SO (Rintoul et al., 2012). In this context, we hope to maintain our observations in the southern Indian Ocean in the next decade, and with ongoing synthetic product activities such as GLODAPv2 (Olsen et al., 2016, 2019), SOCAT (Bakker et al., 2016) and more recently the SOCCOM project (Williams et al., 2018), to offer a solid database to validate ocean biogeochemical models and coupled climate–carbon models (Russell et al., 2018) and ultimately reduce uncertainties in future climate projections.

Data availability. GEOSECS, INDIGO and OISO 1998–2011 data are publicly available via the Ocean Carbon Data System (OCADS; https://www.nodc.noaa.gov/ocads/oceans/GLODAPv2_2019, Olsen et al., 2019). OISO original data are available at https://www.nodc.noaa.gov/ocads/oceans/RepeatSections/clivar_oiso.html (Olsen et al., 2019). OISO 2012–2018 will be available in GLODAPv2.2021.

Supplement. The supplement related to this article is available online at: <https://doi.org/10.5194/os-16-1559-2020-supplement>.

Author contributions. LM, CLM, NM, JF and CM performed the sampling and carried out the measurements of the OISO data. LM prepared the paper with contributions from CLM and NM.

Competing interests. The authors declare that they have no conflict of interest.

Acknowledgements. We thank the captains and crew of the R. S. V. *Marion Dufresne* and the staff at the French Polar Institute (IPEV) for their important contribution to the success of the cruises since 1998. We are also very grateful to all colleagues, students and technicians who helped to obtain the data. We extend our gratitude to Paula Conde Pardo, Steve Rintoul, Benoit Legresy for the discussions during the preparation of the paper and to Megan Kay Shipton for the valuable comments. We thank two anonymous reviewers and the editor Mario Hoppema for their comments and constructive suggestions that helped improve the paper. The OISO program was and is supported by the French institutes INSU, IPEV and OSU Ecce-Terra as well as the French program SOERE/Great-Gases.

Financial support. This research has been supported by the European Integrated Projects CARBOOCEAN (511176) and CARBOCHANGE (264879).

Review statement. This paper was edited by Mario Hoppema and reviewed by two anonymous referees.

References

- Anderson, L. A. and Sarmiento, J. L.: Redfield ratios of remineralization determined by nutrient data analysis, *Global Biogeochem. Cy.*, 8, 65–80, <https://doi.org/10.1029/93gb03318>, 1994.
- Anderson, L. G., Holby, O., Lindegren, R., and Ohlson, M.: The transport of anthropogenic carbon dioxide into the Weddell Sea, *J. Geophys. Res.-Ocean.*, 96, 16679–16687, <https://doi.org/10.1029/91jc01785>, 1991.
- Anilkumar, N., Chacko, R., Sabu, P., and George, J. V.: Freshening of Antarctic Bottom Water in the Indian Ocean sector of Southern Ocean, *Deep-Sea Res. Pt. II*, 118, 162–169, <https://doi.org/10.1016/j.dsr2.2015.03.009>, 2015.
- Bakker, D. C. E., Pfeil, B., Landa, C. S., Metzl, N., O'Brien, K. M., Olsen, A., Smith, K., Cosca, C., Harasawa, S., Jones, S. D., Nakaoka, S., Nojiri, Y., Schuster, U., Steinhoff, T., Sweeney, C., Takahashi, T., Tilbrook, B., Wada, C., Wanninkhof, R., Alin, S. R., Balestrini, C. F., Barbero, L., Bates, N. R., Bianchi, A. A., Bonou, F., Boutin, J., Bozec, Y., Burger, E. F., Cai, W. J., Castle, R. D., Chen, L., Chierici, M., Currie, K., Evans, W., Featherstone, C., Feely, R. A., Fransson, A., Goyet, C., Greenwood, N., Gregor, L., Hankin, S., Hardman-Mountford, N. J., Harlay, J., Hauck, J., Hoppema, M., Humphreys, M. P., Hunt, C. W., Huss, B., Ibáñez, J. S. P., Johannessen, T., Keeling, R., Kitidis, V., Körtzinger, A., Kozyr, A., Krasakopoulou, E., Kuwata, A., Landschützer, P., Lauvset, S. K., Lefèvre, N., Lo Monaco, C., Manke, A., Mathis, J. T., Merlivat, L., Millero, F. J., Monteiro, P. M. S., Munro, D. R., Murata, A., Newberger, T., Omar, A. M., Ono, T., Paterson, K., Pearce, D., Pierrot, D., Robbins, L. L., Saito, S., Salisbury, J., Schlitzer, R., Schneider, B., Schweitzer, R., Sieger, R., Skjelvan, I., Sullivan, K. F., Sutherland, S. C., Sutton, A. J., Tadokoro, K., Telszewski, M., Tuma, M., van Heuven, S. M. A. C., Vandemark, D., Ward, B., Watson, A. J., and Xu, S.: A multi-decade record of high-quality *f*CO₂ data in version 3 of the Surface Ocean CO₂ Atlas (SOCAT), *Earth Syst. Sci. Data*, 8, 383–413, <https://doi.org/10.5194/essd-8-383-2016>, 2016.
- Benson, B. B. and Krause, D.: The concentration and isotopic fractionation of gases dissolved in freshwater in equilibrium with the atmosphere, 1. Oxygen, *Limnol. Oceanogr.*, 25, 662–671, <https://doi.org/10.4319/lo.1980.25.4.0662>, 1980.
- Bockmon, E. E. and Dickson, A. G.: An inter-laboratory comparison assessing the quality of seawater carbon dioxide measurements, *Mar. Chem.*, 171, 36–43, <https://doi.org/10.1016/j.marchem.2015.02.002>, 2015.
- Brewer, P. G.: Direct observation of the oceanic CO₂ increase, *Geophys. Res. Lett.*, 5, 997–1000, <https://doi.org/10.1029/GL005i012p00997>, 1978.
- Broecker, W. S.: “NO”, a conservative water-mass tracer, *Earth Planet. Sc. Lett.*, 23, 100–107, [https://doi.org/10.1016/0012-821X\(74\)90036-3](https://doi.org/10.1016/0012-821X(74)90036-3), 1974.
- Carmack, E. C. and Foster, T. D.: Circulation and distribution of oceanographic properties near the Filchner Ice Shelf, *Deep-Sea Res. Oceanogr. Abstr.*, 22, 77–90, [https://doi.org/10.1016/0011-7471\(75\)90097-2](https://doi.org/10.1016/0011-7471(75)90097-2), 1975.
- Carter, L., McCave, I. N., and Williams, M. J. M.: Chapter 4 Circulation and Water Masses of the Southern Ocean: A Review, in: *Developments in Earth and Environmental Sciences*, edited by: Florindo, F., and Sievert, M., Elsevier, 85–114, [https://doi.org/10.1016/S1571-9197\(08\)00004-9](https://doi.org/10.1016/S1571-9197(08)00004-9), 2008.
- Chen, C.-T. A.: On the distribution of anthropogenic CO₂ in the Atlantic and Southern oceans, *Deep-Sea Res. Pt. A*, 29, 563–580, [https://doi.org/10.1016/0198-0149\(82\)90076-0](https://doi.org/10.1016/0198-0149(82)90076-0), 1982.
- Chen, G.-T. and Millero, F. J.: Gradual increase of oceanic CO₂, *Nature*, 277, 205–206, <https://doi.org/10.1038/277205a0>, 1979.
- Chen, T. and Chen, A.: The oceanic anthropogenic CO₂ sink, *Chemosphere*, 27, 1041–1064, [https://doi.org/10.1016/0045-6535\(93\)90067-F](https://doi.org/10.1016/0045-6535(93)90067-F), 1993.
- Couldrey, M. P., Jullion, L., Naveira Garabato, A. C., Rye, C., Herráiz-Borreguero, L., Brown, P. J., Meredith, M. P., and Speer, K. L.: Remotely induced warming of Antarctic Bottom Water in the eastern Weddell gyre, *Geophys. Res. Lett.*, 40, 2755–2760, <https://doi.org/10.1002/grl.50526>, 2013.
- Coverly, S. C., Aminot, A., and R. Kérouel, 2009. Nutrients in Seawater Using Segmented Flow Analysis, in: *Practical Guidelines for the Analysis of Seawater*, edited by: Oliver Wurl, CRC Press, 143–178, <https://doi.org/10.1201/9781420073072>, 2009.
- De Baar, H. J. W.: Options for enhancing the storage of carbon dioxide in the oceans: A review, *Energ. Convers. Manag.*, 33, 635–642, [https://doi.org/10.1016/0196-8904\(92\)90066-6](https://doi.org/10.1016/0196-8904(92)90066-6), 1992.
- DeJong, H. B. and Dunbar, R. B.: Air-Sea CO₂ Exchange in the Ross Sea, Antarctica, *J. Geophys. Res.-Ocean.*, 122, 8167–8181, <https://doi.org/10.1002/2017JC012853>, 2017.
- Desbruyères, D. G., Purkey, S. G., McDonagh, E. L., Johnson, G. C., and King, B. A.: Deep and abyssal ocean warming from 35 years of repeat hydrography, *Geophys. Res. Lett.*, 43, 10356–10365, <https://doi.org/10.1002/2016GL070413>, 2016.
- DeVries, T., Holzer, M., and Primeau, F.: Recent increase in oceanic carbon uptake driven by weaker upper-ocean overturning, *Nature*, 542, 215–218, <https://doi.org/10.1038/nature21068>, 2017.
- Edmond, J. M.: High precision determination of titration alkalinity and total carbon dioxide content of sea water by potentiometric titration, *Deep-Sea Res. Oceanogr. Abstr.*, 17, 737–750, [https://doi.org/10.1016/0011-7471\(70\)90038-0](https://doi.org/10.1016/0011-7471(70)90038-0), 1970.
- Fahrbach, E., Rohardt, G., Schröder, M., and Strass, V.: Transport and structure of the Weddell Gyre, *Ann. Geophys.*, 12, 840–855, <https://doi.org/10.1007/s00585-994-0840-7>, 1994.
- Fay, A. R., Lovenduski, N. S., McKinley, G. A., Munro, D. R., Sweeney, C., Gray, A. R., Landschützer, P., Stephens, B. B., Takahashi, T., and Williams, N.: Utilizing the Drake Passage Time-series to understand variability and change in sub-polar Southern Ocean *p*CO₂, *Biogeosciences*, 15, 3841–3855, <https://doi.org/10.5194/bg-15-3841-2018>, 2018.
- Frölicher, T. L., Sarmiento, J. L., Paynter, D. J., Dunne, J. P., Krasting, J. P., and Winton, M.: Dominance of the Southern Ocean in Anthropogenic Carbon and Heat Uptake in CMIP5 Models,

- J. Clim., 28, 862–886, <https://doi.org/10.1175/jcli-d-14-00117.1>, 2015.
- Fukamachi, Y., Wakatsuchi, M., Taira, K., Kitagawa, S., Ushio, S., Takahashi, A., Oikawa, K., Furukawa, T., Yoritaka, H., Fukuchi, M., and Yamanouchi, T.: Seasonal variability of bottom water properties off Adélie Land, Antarctica, *J. Geophys. Res.-Ocean.*, 105, 6531–6540, <https://doi.org/10.1029/1999JC900292>, 2000.
- Fukamachi, Y., Rintoul, S. R., Church, J. A., Aoki, S., Sokolov, S., Rosenberg, M. A., and Wakatsuchi, M.: Strong export of Antarctic Bottom Water east of the Kerguelen plateau, *Nat. Geosci.*, 3, 327–331, <https://doi.org/10.1038/ngeo842>, 2010.
- Gattuso, J.-P. and Hansson, L.: *Ocean Acidification*, Oxford University Press, Oxford, New York, 326 pp., 2011.
- Gibson, J. A. E. and Trull, T. W.: Annual cycle of *f*CO₂ under sea-ice and in open water in Prydz Bay, East Antarctica, *Mar. Chem.*, 66, 187–200, [https://doi.org/10.1016/S0304-4203\(99\)00040-7](https://doi.org/10.1016/S0304-4203(99)00040-7), 1999.
- Gordon, A. L.: Bottom Water Formation, in: *Encyclopedia of Ocean Sciences*, Academic Press, © 2019 Elsevier Ltd., 334–340, 2001.
- Gordon, A. L., Orsi, A. H., Muench, R., Huber, B. A., Zambianchi, E., and Visbeck, M.: Western Ross Sea continental slope gravity currents, *Deep-Sea Res. Pt. II*, 56, 796–817, <https://doi.org/10.1016/j.dsr2.2008.10.037>, 2009.
- Gordon, A. L., Huber, B., McKee, D., and Visbeck, M.: A seasonal cycle in the export of bottom water from the Weddell Sea, *Nat. Geosci.*, 3, 551–556, <https://doi.org/10.1038/ngeo916>, 2010.
- Gordon, A. L., Huber, B. A., and Busecke, J.: Bottom water export from the western Ross Sea, 2007 through 2010, *Geophys. Res. Lett.*, 42, 5387–5394, <https://doi.org/10.1002/2015GL064457>, 2015.
- Goyet, C., Adams, R., and Eiseid, G.: Observations of the CO₂ system properties in the tropical Atlantic Ocean, *Mar. Chem.*, 60, 49–61, [https://doi.org/10.1016/S0304-4203\(97\)00081-9](https://doi.org/10.1016/S0304-4203(97)00081-9), 1998.
- Gregor, L., Kok, S., and Monteiro, P. M. S.: Interannual drivers of the seasonal cycle of CO₂ in the Southern Ocean, *Biogeosciences*, 15, 2361–2378, <https://doi.org/10.5194/bg-15-2361-2018>, 2018.
- Gruber, N.: Anthropogenic CO₂ in the Atlantic Ocean, *Global Biogeochem. Cy.*, 12, 165–191, <https://doi.org/10.1029/97GB03658>, 1998.
- Gruber, N., Gloor, M., Mikaloff Fletcher, S. E., Doney, S. C., Dutkiewicz, S., Follows, M. J., Gerber, M., Jacobson, A. R., Joos, F., Lindsay, K., Menemenlis, D., Mouchet, A., Müller, S. A., Sarmiento, J. L., and Takahashi, T.: Oceanic sources, sinks, and transport of atmospheric CO₂, *Global Biogeochem. Cy.*, 23, <https://doi.org/10.1029/2008GB003349>, 2009.
- Gruber, N., Clement, D., Carter, B. R., Feely, R. A., van Heuven, S., Hoppema, M., Ishii, M., Key, R. M., Kozyr, A., Lauvset, S. K., Lo Monaco, C., Mathis, J. T., Murata, A., Olsen, A., Perez, F. F., Sabine, C. L., Tanhua, T., and Wanninkhof, R.: The oceanic sink for anthropogenic CO₂; from 1994 to 2007, *Science*, 363, 1193–1199, <https://doi.org/10.1126/science.aau5153>, 2019a.
- Gruber, N., Landschützer, P., and Lovenduski, N. S.: The Variable Southern Ocean Carbon Sink, *Ann. Rev. Mar. Sci.*, 11, 159–186, <https://doi.org/10.1146/annurev-marine-121916-063407>, 2019b.
- Hauck, J., Völker, C., Wolf-Gladrow, D. A., Laufkötter, C., Vogt, M., Aumont, O., Bopp, L., Buitenhuis, E. T., Doney, S. C., Dunne, J., Gruber, N., Hashioka, T., John, J., Quéré, C. L., Lima, I. D., Nakano, H., Séférian, R., and Totterdell, I.: On the Southern Ocean CO₂ uptake and the role of the biological carbon pump in the 21st century, *Global Biogeochem. Cy.*, 29, 1451–1470, <https://doi.org/10.1002/2015GB005140>, 2015.
- Heuzé, C., Heywood, K. J., Stevens, D. P., and Ridley, J. K.: Changes in Global Ocean Bottom Properties and Volume Transports in CMIP5 Models under Climate Change Scenarios, *J. Clim.*, 28, 2917–2944, <https://doi.org/10.1175/JCLI-D-14-00381.1>, 2015.
- Heywood, K. J., Sparrow, M. D., Brown, J., and Dickson, R. R.: Frontal structure and Antarctic Bottom Water flow through the Princess Elizabeth Trough, Antarctica, *Deep-Sea Res. Pt. I*, 46, 1181–1200, [https://doi.org/10.1016/S0967-0637\(98\)00108-3](https://doi.org/10.1016/S0967-0637(98)00108-3), 1999.
- Ito, T., Bracco, A., Deutsch, C., Frenzel, H., Long, M., and Takano, Y.: Sustained growth of the Southern Ocean carbon storage in a warming climate, *Geophys. Res. Lett.*, 42, 4516–4522, <https://doi.org/10.1002/2015GL064320>, 2015.
- Jabaud-Jan, A., Metzl, N., Brunet, C., Poisson, A., and Schauer, B.: Interannual variability of the carbon dioxide system in the southern Indian Ocean (20° S–60° S): The impact of a warm anomaly in austral summer 1998, *Global Biogeochem. Cy.*, 18, GB1042, <https://doi.org/10.1029/2002GB002017>, 2004.
- Jiang, L.-Q., Carter, B. R., Feely, R. A., Lauvset, S. K., and Olsen, A.: Surface ocean pH and buffer capacity: past, present and future, *Sci. Rep.*, 9, 18624, <https://doi.org/10.1038/s41598-019-55039-4>, 2019.
- Johnson, G. C.: Quantifying Antarctic Bottom Water and North Atlantic Deep Water volumes, *J. Geophys. Res.-Ocean.*, 113, C05027, <https://doi.org/10.1029/2007JC004477>, 2008.
- Johnson, G. C., Purkey, S. G., and Bullister, J. L.: Warming and Freshening in the Abyssal Southeastern Indian Ocean, *J. Clim.*, 21, 5351–5363, <https://doi.org/10.1175/2008JCLI2384.1>, 2008.
- Keeling, C. D. and Whorf, T. P.: Monthly carbon dioxide measurements on Mauna Loa, Hawaii from 1958 to 1998, PANGAEA, <https://doi.org/10.1594/PANGAEA.56536>, 2000.
- Kerr, R., Goyet, C., da Cunha, L. C., Orselli, I. B. M., Lencina-Avila, J. M., Mendes, C. R. B., Carvalho-Borges, M., Mata, M. M., and Tavano, V. M.: Carbonate system properties in the Gerlache Strait, Northern Antarctic Peninsula (February 2015): II. Anthropogenic CO₂ and seawater acidification, *Deep-Sea Res. Pt. II*, 149, 182–192, <https://doi.org/10.1016/j.dsr2.2017.07.007>, 2018.
- Key, R. M., Kozyr, A., Sabine, C. L., Lee, K., Wanninkhof, R., Bullister, J. L., Feely, R. A., Millero, F. J., Mordy, C., and Peng, T. H.: A global ocean carbon climatology: Results from Global Data Analysis Project (GLODAP), *Global Biogeochem. Cy.*, 18, GB4031, <https://doi.org/10.1029/2004GB002247>, 2004.
- Key, R. M., Olsen, A., Van Heuven, S., Lauvset, S. K., Velo, A., Lin, X., Schirnick, C., Kozyr, A., Tanhua, T., Hoppema, M., Jutterstrom, S., Steinfeldt, R., Jeansson, E., Ishi, M., Perez, F. F., and Suzuki, T.: Global Ocean Data Analysis Project, Version 2 (GLODAPv2), ORNL/CDIAC-162, ND-P093, https://doi.org/10.3334/CDIAC/OTG.NDP093_GLODAPv2, 2015.
- Khatiwala, S., Primeau, F., and Hall, T.: Reconstruction of the history of anthropogenic CO₂ concentrations in the ocean, *Nature*, 462, 346–349, <https://doi.org/10.1038/nature08526>, 2009.
- Khatiwala, S., Tanhua, T., Mikaloff Fletcher, S., Gerber, M., Doney, S. C., Graven, H. D., Gruber, N., McKinley, G. A.,

- Murata, A., Ríos, A. F., and Sabine, C. L.: Global ocean storage of anthropogenic carbon, *Biogeosciences*, 10, 2169–2191, <https://doi.org/10.5194/bg-10-2169-2013>, 2013.
- Körtzinger, A., Mintrop, L., and Duinker, J. C.: On the penetration of anthropogenic CO₂ into the North Atlantic Ocean, *J. Geophys. Res.-Ocean.*, 103, 18681–18689, <https://doi.org/10.1029/98JC01737>, 1998.
- Körtzinger, A., Rhein, M., and Mintrop, L.: Anthropogenic CO₂ and CFCs in the North Atlantic Ocean – A comparison of man-made tracers, *Geophys. Res. Lett.*, 26, 2065–2068, <https://doi.org/10.1029/1999GL900432>, 1999.
- Körtzinger, A., Hedges, J. I., and Quay, P. D.: Redfield ratios revisited: Removing the biasing effect of anthropogenic CO₂, *Limnol. Oceanogr.*, 46, 964–970, <https://doi.org/10.4319/lo.2001.46.4.0964>, 2001.
- Landschützer, P., Gruber, N., Haumann, F. A., Rödenbeck, C., Bakker, D. C. E., van Heuven, S., Hoppema, M., Metzl, N., Sweeney, C., Takahashi, T., Tilbrook, B., and Wanninkhof, R.: The reinvigoration of the Southern Ocean carbon sink, *Science*, 349, 1221–1224, <https://doi.org/10.1126/science.aab2620>, 2015.
- Laruelle, G. G., Cai, W.-J., Hu, X., Gruber, N., Mackenzie, F. T., and Regnier, P.: Continental shelves as a variable but increasing global sink for atmospheric carbon dioxide, *Nat. Commun.*, 9, 454, <https://doi.org/10.1038/s41467-017-02738-z>, 2018.
- Lenton, A., Codron, F., Bopp, L., Metzl, N., Cadule, P., Tagliabue, A., and Le Sommer, J.: Stratospheric ozone depletion reduces ocean carbon uptake and enhances ocean acidification, *Geophys. Res. Lett.*, 36, L12606, <https://doi.org/10.1029/2009GL038227>, 2009.
- Le Quéré, C., Rödenbeck, C., Buitenhuis, E. T., Conway, T. J., Langenfelds, R., Gomez, A., Labuschagne, C., Ramonet, M., Nakazawa, T., Metzl, N., Gillett, N., and Heimann, M.: Saturation of the Southern Ocean CO₂; Sink Due to Recent Climate Change, *Science*, 316, 1735–1738, <https://doi.org/10.1126/science.1136188>, 2007.
- Le Quéré, C., Andrew, R. M., Friedlingstein, P., Sitch, S., Hauck, J., Pongratz, J., Pickers, P. A., Korsbakken, J. I., Peters, G. P., Canadell, J. G., Arneeth, A., Arora, V. K., Barbero, L., Bastos, A., Bopp, L., Chevallier, F., Chini, L. P., Ciais, P., Doney, S. C., Gkritzalis, T., Goll, D. S., Harris, I., Haverd, V., Hoffman, F. M., Hoppema, M., Houghton, R. A., Hurtt, G., Ilyina, T., Jain, A. K., Johannessen, T., Jones, C. D., Kato, E., Keeling, R. F., Goldewijk, K. K., Landschützer, P., Lefèvre, N., Lienert, S., Liu, Z., Lombardozi, D., Metzl, N., Munro, D. R., Nabel, J. E. M. S., Nakaoka, S., Neill, C., Olsen, A., Ono, T., Patra, P., Peregón, A., Peters, W., Peylin, P., Pfeil, B., Pierrot, D., Poulter, B., Rehder, G., Resplandy, L., Robertson, E., Rocher, M., Rödenbeck, C., Schuster, U., Schwinger, J., Séférian, R., Skjelvan, I., Steinhoff, T., Sutton, A., Tans, P. P., Tian, H., Tilbrook, B., Tubiello, F. N., van der Laan-Luijckx, I. T., van der Werf, G. R., Viovy, N., Walker, A. P., Wiltshire, A. J., Wright, R., Zaehle, S., and Zheng, B.: Global Carbon Budget 2018, *Earth Syst. Sci. Data*, 10, 2141–2194, <https://doi.org/10.5194/essd-10-2141-2018>, 2018.
- Lenton, A., Metzl, N., Takahashi, T., Kuchinke, M., Matear, R. J., Roy, T., Sutherland, S. C., Sweeney, C., and Tilbrook, B.: The observed evolution of oceanic *p*CO₂ and its drivers over the last two decades, *Global Biogeochem. Cy.*, 26, GB2021, <https://doi.org/10.1029/2011GB004095>, 2012.
- Lo Monaco, C., Goyet, C., Metzl, N., Poisson, A., and Touratier, F.: Distribution and inventory of anthropogenic CO₂ in the Southern Ocean: Comparison of three data-based methods, *J. Geophys. Res.-Ocean.*, 110, C09S02, <https://doi.org/10.1029/2004JC002571>, 2005a.
- Lo Monaco, C., Metzl, N., Poisson, A., Brunet, C., and Schauer, B.: Anthropogenic CO₂ in the Southern Ocean: Distribution and inventory at the Indian-Atlantic boundary (World Ocean Circulation Experiment line I6), *J. Geophys. Res.-Ocean.*, 110, C06010, <https://doi.org/10.1029/2004JC002643>, 2005b.
- Lo Monaco, C., Álvarez, M., Key, R. M., Lin, X., Tanhua, T., Tilbrook, B., Bakker, D. C. E., van Heuven, S., Hoppema, M., Metzl, N., Ríos, A. F., Sabine, C. L., and Velo, A.: Assessing the internal consistency of the CARINA database in the Indian sector of the Southern Ocean, *Earth Syst. Sci. Data*, 2, 51–70, <https://doi.org/10.5194/essd-2-51-2010>, 2010.
- Mantyla, A. W. and Reid, J. L.: On the origins of deep and bottom waters of the Indian Ocean, *J. Geophys. Res.-Ocean.*, 100, 2417–2439, <https://doi.org/10.1029/94JC02564>, 1995.
- Marshall, J. and Speer, K.: Closure of the meridional overturning circulation through Southern Ocean upwelling, *Nat. Geosci.*, 5, 171–180, <https://doi.org/10.1038/ngeo1391>, 2012.
- Matear, R. J.: Effects of numerical advection schemes and eddy parameterizations on ocean ventilation and oceanic anthropogenic CO₂ uptake, *Ocean Model.*, 3, 217–248, [https://doi.org/10.1016/S1463-5003\(01\)00010-5](https://doi.org/10.1016/S1463-5003(01)00010-5), 2001.
- McKee, D. C., Yuan, X., Gordon, A. L., Huber, B. A., and Dong, Z.: Climate impact on interannual variability of Weddell Sea Bottom Water, *J. Geophys. Res.-Ocean.*, 116, C05020, <https://doi.org/10.1029/2010JC006484>, 2011.
- McNeil, B. I., Matear, R. J., Key, R. M., Bullister, J. L., and Sarmiento, J. L.: Anthropogenic CO₂ Uptake by the Ocean Based on the Global Chlorofluorocarbon Data Set, *Science*, 299, 235–239, <https://doi.org/10.1126/science.1077429>, 2003.
- Meijers, A. J. S., Klocker, A., Bindoff, N. L., Williams, G. D., and Marsland, S. J.: The circulation and water masses of the Antarctic shelf and continental slope between 30 and 80° E, *Deep-Sea Res. Pt. II*, 57, 723–737, <https://doi.org/10.1016/j.dsr2.2009.04.019>, 2010.
- Menezes, V. V., Macdonald, A. M., and Schatzman, C.: Accelerated freshening of Antarctic Bottom Water over the last decade in the Southern Indian Ocean, *Sci. Adv.*, 3, e1601426, <https://doi.org/10.1126/sciadv.1601426>, 2017.
- Metzl, N.: Decadal increase of oceanic carbon dioxide in Southern Indian Ocean surface waters (1991–2007), *Deep-Sea Res. Pt. II*, 56, 607–619, <https://doi.org/10.1016/j.dsr2.2008.12.007>, 2009.
- Metzl, N., Brunet, C., Jabaud-Jan, A., Poisson, A., and Schauer, B.: Summer and winter air–sea CO₂ fluxes in the Southern Ocean, *Deep-Sea Res. Pt. I*, 53, 1548–1563, <https://doi.org/10.1016/j.dsr.2006.07.006>, 2006.
- Munro, D. R., Lovenduski, N. S., Takahashi, T., Stephens, B. B., Newberger, T., and Sweeney, C.: Recent evidence for a strengthening CO₂ sink in the Southern Ocean from carbonate system measurements in the Drake Passage (2002–2015), *Geophys. Res. Lett.*, 42, 7623–7630, <https://doi.org/10.1002/2015GL065194>, 2015.
- Murata, A., Kumamoto, Y.-i., and Sasaki, K.-i.: Decadal-Scale Increases of Anthropogenic CO₂ in Antarctic Bottom Water in the Indian and Western Pacific Sectors of

- the Southern Ocean, *Geophys. Res. Lett.*, 46, 833–841, <https://doi.org/10.1029/2018GL080604>, 2019.
- Ohshima, K. I., Fukamachi, Y., Williams, G. D., Nihashi, S., Roquet, F., Kitade, Y., Tamura, T., Hirano, D., Herraiz-Borreguero, L., Field, I., Hindell, M., Aoki, S., and Wakatsuchi, M.: Antarctic Bottom Water production by intense sea-ice formation in the Cape Darnley polynya, *Nat. Geosci.*, 6, 235–240, <https://doi.org/10.1038/ngeo1738>, 2013.
- Olsen, A., Key, R. M., van Heuven, S., Lauvset, S. K., Velo, A., Lin, X., Schirnick, C., Kozyr, A., Tanhua, T., Hoppema, M., Jutterström, S., Steinfeldt, R., Jeansson, E., Ishii, M., Pérez, F. F., and Suzuki, T.: The Global Ocean Data Analysis Project version 2 (GLODAPv2) – an internally consistent data product for the world ocean, *Earth Syst. Sci. Data*, 8, 297–323, <https://doi.org/10.5194/essd-8-297-2016>, 2016.
- Olsen, A., Lange, N., Key, R. M., Tanhua, T., Álvarez, M., Becker, S., Bittig, H. C., Carter, B. R., Cotrim da Cunha, L., Feely, R. A., van Heuven, S., Hoppema, M., Ishii, M., Jeansson, E., Jones, S. D., Jutterström, S., Karlsen, M. K., Kozyr, A., Lauvset, S. K., Lo Monaco, C., Murata, A., Pérez, F. F., Pfeil, B., Schirnick, C., Steinfeldt, R., Suzuki, T., Telszewski, M., Tilbrook, B., Velo, A., and Wanninkhof, R.: GLODAPv2.2019 – an update of GLODAPv2, *Earth Syst. Sci. Data*, 11, 1437–1461, <https://doi.org/10.5194/essd-11-1437-2019>, 2019.
- Orr, J. C., Maier-Reimer, E., Mikolajewicz, U., Monfray, P., Sarmiento, J. L., Toggweiler, J. R., Taylor, N. K., Palmer, J., Gruber, N., Sabine, C. L., Le Quééré, C., Key, R. M., and Boutin, J.: Estimates of anthropogenic carbon uptake from four three-dimensional global ocean models, *Global Biogeochem. Cy.*, 15, 43–60, <https://doi.org/10.1029/2000GB001273>, 2001.
- Orr, J. C., Fabry, V. J., Aumont, O., Bopp, L., Doney, S. C., Feely, R. A., Gnanadesikan, A., Gruber, N., Ishida, A., Joos, F., Key, R. M., Lindsay, K., Maier-Reimer, E., Matear, R., Monfray, P., Mouchet, A., Najjar, R. G., Plattner, G.-K., Rodgers, K. B., Sabine, C. L., Sarmiento, J. L., Schlitzer, R., Slater, R. D., Totterdell, I. J., Weirig, M.-F., Yamanaka, Y., and Yool, A.: Anthropogenic ocean acidification over the twenty-first century and its impact on calcifying organisms, *Nature*, 437, 681–686, <https://doi.org/10.1038/nature04095>, 2005.
- Orsi, A. H., Johnson, G. C., and Bullister, J. L.: Circulation, mixing, and production of Antarctic Bottom Water, *Prog. Oceanogr.*, 43, 55–109, [https://doi.org/10.1016/S0079-6611\(99\)00004-X](https://doi.org/10.1016/S0079-6611(99)00004-X), 1999.
- Pardo, P. C., Pérez, F. F., Khatiwala, S., and Ríos, A. F.: Anthropogenic CO₂ estimates in the Southern Ocean: Storage partitioning in the different water masses, *Prog. Oceanogr.*, 120, 230–242, <https://doi.org/10.1016/j.pocean.2013.09.005>, 2014.
- Pardo, P. C., Tilbrook, B., Langlais, C., Trull, T. W., and Rintoul, S. R.: Carbon uptake and biogeochemical change in the Southern Ocean, south of Tasmania, *Biogeosciences*, 14, 5217–5237, <https://doi.org/10.5194/bg-14-5217-2017>, 2017.
- Poisson, A. and Chen, C.-T. A.: Why is there little anthropogenic CO₂ in the Antarctic bottom water?, *Deep-Sea Res. Pt. A*, 34, 1255–1275, [https://doi.org/10.1016/0198-0149\(87\)90075-6](https://doi.org/10.1016/0198-0149(87)90075-6), 1987.
- Purkey, S. G. and Johnson, G. C.: Warming of Global Abyssal and Deep Southern Ocean Waters between the 1990s and 2000s: Contributions to Global Heat and Sea Level Rise Budgets, *J. Clim.*, 23, 6336–6351, <https://doi.org/10.1175/2010JCLI3682.1>, 2010.
- Purkey, S. G. and Johnson, G. C.: Global Contraction of Antarctic Bottom Water between the 1980s and 2000s, *J. Clim.*, 25, 5830–5844, <https://doi.org/10.1175/JCLI-D-11-00612.1>, 2012.
- Ridgwell, A. and Zeebe, R. E.: The role of the global carbonate cycle in the regulation and evolution of the Earth system, *Earth Planet. Sc. Lett.*, 234, 299–315, <https://doi.org/10.1016/j.epsl.2005.03.006>, 2005.
- Rintoul, S. R.: Rapid freshening of Antarctic Bottom Water formed in the Indian and Pacific oceans, *Geophys. Res. Lett.*, 34, L06606, <https://doi.org/10.1029/2006GL028550>, 2007.
- Rintoul, S. R., Sparrow, M., Meredith, M. P., Wadley, V., Speer, K., Hofmann, E., Summerhayes, C., Urban, E., and Bellerby, R.: The Southern Ocean Observing System: Initial Science and Implementation Strategy, Scientific Committee on Antarctic Research/Scientific Committee on Oceanic Research, 74 pp., 2012.
- Ríos, A. F., Velo, A., Pardo, P. C., Hoppema, M., and Pérez, F. F.: An update of anthropogenic CO₂ storage rates in the western South Atlantic basin and the role of Antarctic Bottom Water, *J. Mar. Syst.*, 94, 197–203, <https://doi.org/10.1016/j.jmarsys.2011.11.023>, 2012.
- Robertson, R., Visbeck, M., Gordon, A. L., and Fahrback, E.: Long-term temperature trends in the deep waters of the Weddell Sea, *Deep-Sea Res. Pt. II*, 49, 4791–4806, [https://doi.org/10.1016/S0967-0645\(02\)00159-5](https://doi.org/10.1016/S0967-0645(02)00159-5), 2002.
- Rodehacke, C. B., Hellmer, H. H., Beckmann, A., and Roether, W.: Formation and spreading of Antarctic deep and bottom waters inferred from a chlorofluorocarbon (CFC) simulation, *J. Geophys. Res.-Ocean.*, 112, C09001, <https://doi.org/10.1029/2006JC003884>, 2007.
- Roden, N. P., Shadwick, E. H., Tilbrook, B., and Trull, T. W.: Annual cycle of carbonate chemistry and decadal change in coastal Prydz Bay, East Antarctica, *Mar. Chem.*, 155, 135–147, <https://doi.org/10.1016/j.marchem.2013.06.006>, 2013.
- Roden, N. P., Tilbrook, B., Trull, T. W., Virtue, P., and Williams, G. D.: Carbon cycling dynamics in the seasonal sea-ice zone of East Antarctica, *J. Geophys. Res.-Ocean.*, 121, 8749–8769, <https://doi.org/10.1002/2016JC012008>, 2016.
- Russell, J. L., Kamenkovich, I., Bitz, C., Ferrari, R., Gille, S. T., Goodman, P. J., Hallberg, R., Johnson, K., Khazmutdinova, K., Marinov, I., Mazloff, M., Riser, S., Sarmiento, J. L., Speer, K., Talley, L. D., and Wanninkhof, R.: Metrics for the Evaluation of the Southern Ocean in Coupled Climate Models and Earth System Models, *J. Geophys. Res.-Ocean.*, 123, 3120–3143, <https://doi.org/10.1002/2017JC013461>, 2018.
- Sabine, C. L., Key, R. M., Johnson, K. M., Millero, F. J., Poisson, A., Sarmiento, J. L., Wallace, D. W. R., and Winn, C. D.: Anthropogenic CO₂ inventory of the Indian Ocean, *Global Biogeochem. Cy.*, 13, 179–198, <https://doi.org/10.1029/1998GB900022>, 1999.
- Sabine, C. L., Feely, R. A., Gruber, N., Key, R. M., Lee, K., Bullister, J. L., Wanninkhof, R., Wong, C. S., Wallace, D. W. R., Tilbrook, B., Millero, F. J., Peng, T.-H., Kozyr, A., Ono, T., and Ríos, A. F.: The Oceanic Sink for Anthropogenic CO₂, *Science*, 305, 367–371, <https://doi.org/10.1126/science.1097403>, 2004.
- Sandrini, S., Ait-Ameur, N., Rivaro, P., Massolo, S., Touratier, F., Tositti, L., and Goyet, C.: Anthropogenic carbon distribution in the Ross Sea, Antarctica, *Antarct. Sci.*, 19, 395–407, <https://doi.org/10.1017/S0954102007000405>, 2007.

- Schlitzer, R.: Ocean Data View, available at: <http://odv.awi.de>, last access: 2 September 2019.
- Schmidtko, S., Stramma, L., and Visbeck, M.: Decline in global oceanic oxygen content during the past five decades, *Nature*, 542, 335–339, <https://doi.org/10.1038/nature21399>, 2017.
- Shadwick, E. H., Rintoul, S. R., Tilbrook, B., Williams, G. D., Young, N., Fraser, A. D., Marchant, H., Smith, J., and Tamura, T.: Glacier tongue calving reduced dense water formation and enhanced carbon uptake, *Geophys. Res. Lett.*, 40, 904–909, <https://doi.org/10.1002/grl.50178>, 2013.
- Shadwick, E. H., Tilbrook, B., and Williams, G. D.: Carbonate chemistry in the Mertz Polynya (East Antarctica): Biological and physical modification of dense water outflows and the export of anthropogenic CO₂, *J. Geophys. Res.-Ocean.*, 119, 1–14, <https://doi.org/10.1002/2013JC009286>, 2014.
- Siegenthaler, U. and Sarmiento, J. L.: Atmospheric carbon dioxide and the ocean, *Nature*, 365, 119–125, <https://doi.org/10.1038/365119a0>, 1993.
- Smith, N. and Treguer, P.: Physical and Chemical Oceanography in the Vicinity of Prydz Bay, Antarctica, edited by: ElSayed, S. Z., Cambridge Univ Press, Cambridge, 25–43, 1994.
- Swart, N. C., Gille, S. T., Fyfe, J. C., and Gillett, N. P.: Recent Southern Ocean warming and freshening driven by greenhouse gas emissions and ozone depletion, *Nat. Geosci.*, 11, 836–841, <https://doi.org/10.1038/s41561-018-0226-1>, 2018.
- Takahashi, T., Sutherland, S. C., Wanninkhof, R., Sweeney, C., Feely, R. A., Chipman, D. W., Hales, B., Friederich, G., Chavez, F., Sabine, C., Watson, A., Bakker, D. C. E., Schuster, U., Metzl, N., Yoshikawa-Inoue, H., Ishii, M., Midorikawa, T., Nojiri, Y., Körtzinger, A., Steinhoff, T., Hoppema, M., Olafsson, J., Arnarson, T. S., Tilbrook, B., Johannessen, T., Olsen, A., Bellerby, R., Wong, C. S., Delille, B., Bates, N. R., and de Baar, H. J. W.: Climatological mean and decadal change in surface ocean pCO₂, and net sea–air CO₂ flux over the global oceans, *Deep-Sea Res. Pt. II*, 56, 554–577, <https://doi.org/10.1016/j.dsr2.2008.12.009>, 2009.
- Takahashi, T., Sweeney, C., Hales, B., Chipman, D. W., Newberger, T., Goddard, J. G., Iannuzzi, R. A., and Sutherland, S. C.: The Changing Carbon Cycle in the Southern Ocean, *Oceanography*, 25, 26–37, 2012.
- Tamura, T., Ohshima, K. I., Fraser, A. D., and Williams, G. D.: Sea ice production variability in Antarctic coastal polynyas, *J. Geophys. Res.-Ocean.*, 121, 2967–2979, <https://doi.org/10.1002/2015JC011537>, 2016.
- Touratier, F. and Goyet, C.: Definition, properties, and Atlantic Ocean distribution of the new tracer TrOCA, *J. Mar. Syst.*, 46, 169–179, <https://doi.org/10.1016/j.jmarsys.2003.11.016>, 2004a.
- Touratier, F. and Goyet, C.: Applying the new TrOCA approach to assess the distribution of anthropogenic CO₂ in the Atlantic Ocean, *J. Mar. Syst.*, 46, 181–197, <https://doi.org/10.1016/j.jmarsys.2003.11.020>, 2004b.
- Touratier, F., Azouzi, L., and Goyet, C.: CFC-11, $\Delta^{14}\text{C}$ and ^3H tracers as a means to assess anthropogenic CO₂ concentrations in the ocean, *Tellus B*, 59, 318–325, <https://doi.org/10.1111/j.1600-0889.2006.00247.x>, 2007.
- Tréguer, P. and Le Corre, P.: Manuel d'analyse des sels nutritifs dans l'eau de mer (utilisation de l'autoanalyseur II Technicon), 2nd Edn., L.O.C.U.B.O., Brest, 110 pp., 1975.
- van Heuven, S. M. A. C., Hoppema, M., Huhn, O., Slagter, H. A., and de Baar, H. J. W.: Direct observation of increasing CO₂ in the Weddell Gyre along the Prime Meridian during 1973–2008, *Deep-Sea Res. Pt. II*, 58, 2613–2635, <https://doi.org/10.1016/j.dsr2.2011.08.007>, 2011.
- van Heuven, S. M. A. C.: Determination of the rate of oceanic storage of anthropogenic CO₂ from measurements in the ocean interior: The South Atlantic Ocean, Doctor of Philosophy, Groningen, 268 pp., 2013.
- van Heuven, S. M. A. C., Hoppema, M., Jones, E. M., and de Baar, H. J. W.: Rapid invasion of anthropogenic CO₂ into the deep circulation of the Weddell Gyre, *Philos. T. R. Soc. A*, 372, 20130056, <https://doi.org/10.1098/rsta.2013.0056>, 2014.
- van Wijk, E. M. and Rintoul, S. R.: Freshening drives contraction of Antarctic Bottom Water in the Australian Antarctic Basin, *Geophys. Res. Lett.*, 41, 1657–1664, <https://doi.org/10.1002/2013GL058921>, 2014.
- Vázquez-Rodríguez, M., Touratier, F., Lo Monaco, C., Waugh, D. W., Padin, X. A., Bellerby, R. G. J., Goyet, C., Metzl, N., Ríos, A. F., and Pérez, F. F.: Anthropogenic carbon distributions in the Atlantic Ocean: data-based estimates from the Arctic to the Antarctic, *Biogeosciences*, 6, 439–451, <https://doi.org/10.5194/bg-6-439-2009>, 2009.
- Vernet, M., Geibert, W., Hoppema, M., Brown, P. J., Haas, C., Hellmer, H. H., Jokat, W., Jullion, L., Mazloff, M., Bakker, D. C. E., Brearley, J. A., Croot, P., Hattermann, T., Hauck, J., Hillenbrand, C. D., Hoppe, C. J. M., Huhn, O., Koch, B. P., Lechtenfeld, O. J., Meredith, M. P., Naveira Garabato, A. C., Nöthig, E. M., Peeken, I., Rutgers van der Loeff, M. M., Schmidtko, S., Schröder, M., Strass, V. H., Torres-Valdés, S., and Verdy, A.: The Weddell Gyre, Southern Ocean: Present Knowledge and Future Challenges, *Rev. Geophys.*, 57, 623–708, <https://doi.org/10.1029/2018RG000604>, 2019.
- Waugh, D. W., Hall, T. M., McNeil, B. I., Key, R., and Matear, R. J.: Anthropogenic CO₂ in the oceans estimated using transit time distributions, *Tellus B*, 58, 376–389, <https://doi.org/10.1111/j.1600-0889.2006.00222.x>, 2006.
- Weiss, R. F.: The solubility of nitrogen, oxygen and argon in water and seawater, *Deep-Sea Res. Oceanogr. Abstracts*, 17, 721–735, [https://doi.org/10.1016/0011-7471\(70\)90037-9](https://doi.org/10.1016/0011-7471(70)90037-9), 1970.
- Williams, W. J., Carmack, E. C., and Ingram, R. G.: Physical oceanography of polynyas, *Elsevier Oceanography Series*, 74, 55–85, [https://doi.org/10.1016/S0422-9894\(06\)74002-8](https://doi.org/10.1016/S0422-9894(06)74002-8), 2007.
- Williams, G. D., Bindoff, N. L., Marsland, S. J., and Rintoul, S. R.: Formation and export of dense shelf water from the Adélie Depression, East Antarctica, *J. Geophys. Res.-Ocean.*, 113, C04039, <https://doi.org/10.1029/2007JC004346>, 2008.
- Williams, G. D., Aoki, S., Jacobs, S. S., Rintoul, S. R., Tamura, T., and Bindoff, N. L.: Antarctic Bottom Water from the Adélie and George V Land coast, East Antarctica (140–149° E), *J. Geophys. Res.-Ocean.*, 115, C04027, <https://doi.org/10.1029/2009JC005812>, 2010.
- Williams, G. D., Herraiz-Borreguero, L., Roquet, F., Tamura, T., Ohshima, K. I., Fukamachi, Y., Fraser, A. D., Gao, L., Chen, H., McMahon, C. R., Harcourt, R., and Hindell, M.: The suppression of Antarctic bottom water formation by melting ice shelves in Prydz Bay, *Nat. Commun.*, 7, 12577, <https://doi.org/10.1038/ncomms12577>, 2016.

- Williams, N. L., Feely, R. A., Sabine, C. L., Dickson, A. G., Swift, J. H., Talley, L. D., and Russell, J. L.: Quantifying anthropogenic carbon inventory changes in the Pacific sector of the Southern Ocean, *Mar. Chem.*, 174, 147–160, <https://doi.org/10.1016/j.marchem.2015.06.015>, 2015.
- Williams, N. L., Juranek, L. W., Feely, R. A., Russell, J. L., Johnson, K. S., and Hales, B.: Assessment of the Carbonate Chemistry Seasonal Cycles in the Southern Ocean From Persistent Observational Platforms, *J. Geophys. Res.-Ocean.*, 123, 4833–4852, <https://doi.org/10.1029/2017JC012917>, 2018.
- Yabuki, T., Suga, T., Hanawa, K., Matsuoka, K., Kiwada, H., and Watanabe, T.: Possible source of the antarctic bottom water in the Prydz Bay Region, *J. Oceanogr.*, 62, 649–655, <https://doi.org/10.1007/s10872-006-0083-1>, 2006.
- Yamamoto, A., Abe-Ouchi, A., Shigemitsu, M., Oka, A., Takahashi, K., Ohgaito, R., and Yamanaka, Y.: Global deep ocean oxygenation by enhanced ventilation in the Southern Ocean under long-term global warming, *Global Biogeochem. Cy.*, 29, 1801–1815, <https://doi.org/10.1002/2015GB005181>, 2015.